Comparison of ANSYS elements SHELL181 and SOLSH190

Biswajit Banerjee[1]

18 July, 2011

[1] b.banerjee.nz@gmail.com, Industrial Research Limited, NZ

Contents

Abstract

Plate and shell elements are indispensable for the study of the mechanics of complex structures. Two classes of shell elements are commonly used in finite element analyses of thin structures, classical two-dimensional elements and three-dimensional continuum elements. Users of commercial finite element software, such as ANSYS[TM], are often unsure of the relative strengths and weaknesses of these elements and of the appropriate use of these elements. This report provides data that can be used as a basis for the selection of shell elements for engineering analysis and design. The displacements and stresses predicted by two ANSYS[TM] shell elements, SHELL181 and SOLSH190, are compared with exact solutions and full three-dimensional simulations for several geometries and boundary conditions. We conclude that classical shell, SHELL181, elements and solid shell, SOLSH190, elements behave in a similar, though not identical, manner for many situations. For instance, SHELL181 elements generate poor solutions compared to SOLSH190 elements for sandwich plates with isotropic layers and small core to facesheet stiffness ratios. However, for low stiffness cores of moderately high shear stiffness, both SHELL181 and SOLSH190 elements perform adequately. We also note that plates modeled with a single layer of SOLSH190 elements are extremely stiff in bending and we recommend at least three elements through the plate thickness for reasonable results. Also, boundary conditions have to be applied to all the nodes of SOLSH190 elements to achieve the correct mid-surface deformation behavior. The solid shell element provided by ANSYS[TM] can be used to replace standard shell elements provided care is taken during its use.

1 Introduction

A search of the web pages that discuss finite element software packages often brings up the issue of using "solid shell" elements. Questions typically involve the correct number of elements through the thickness, means of attaching these elements to three-dimensional "solid" elements, applicability of complex constitutive models when using these elements, and so on. Users typically seek to use solid shell elements because of the potentially lower cost (in terms of pre-processing time) in moving from a CAD geometry to a finite element model when these elements are used.

Classical shell elements are two-dimensional and the geometry represents the mid-surface (though other reference surfaces may be used) of a relatively thin three-dimensional structure. Since CAD geometries are typically three dimensional, thin objects have to be preprocessed so that the mid-surface can be extracted and joined to neighbouring structures (which may themselves be shells or three-dimensional solids). This preprocessing step can be tedious and fraught with errors and the avoidance of this process appears to be the driving force towards migration to solid shell elements.

Since solid shells are three-dimensional, it should in principle be easier to directly map CAD geometries to these elements. However, though a voluminous literature on the behavior of these elements exists, the implementation can vary between software vendors and the applicability of existing results from the literature is often in doubt.

The aim of this study is to explore the viability of replacing the classical ANSYS[TM] shell element, SHELL181, with SOLSH190 elements. Only geometrically and materially linear computations are considered. Special emphasis has been placed on sandwich structures with stiff facesheets and soft cores. We have examined the elements provided in versions 11, 12.1, and 13 of ANSYS[TM].

The study starts with an examination of classical plate theory solutions for simply supported isotropic plates under uniform pressure and boundary moments. This is followed by a study of cantilever plates, exact solutions for which are rare and usually incomplete for finite plates. Isotropic and orthotropic cantilevered plates are examined first, followed by cantilevered sandwich plates loaded by concentrated edge loads. Finally, the important case of a cantilevered plate under a body force load is examined.

Displacements and stresses are plotted for the various situations explored in this study. In addi-

tion, we also plot a quantity that is called the percent difference, defined as

$$\text{Difference(\%)} = \frac{\text{ANSYS solution} - \text{Exact solution}}{\text{ANSYS solution}} \times 100\,.$$

For situations where an exact solution does not exist, the percent difference is defined as

$$\text{Difference(\%)} = \frac{\text{ANSYS solution} - \text{ANSYS SOLID185 solution}}{\text{ANSYS solution}} \times 100$$

where a converged solution using linear three-dimensional SOLID185 elements is assumed to be the "accurate" solution. The plots shown in the report suggest that this assumption is reasonable.

2 Simply supported isotropic plate under uniform load

Consider a square plate of length 1 m, width 1 m which is made of an isotropic material with Young's modulus 200 GPa and Poisson's ratio 0.27. In this section, predictions from ANSYS$^{\text{TM}}$ are compared with exact solutions for a pressure load of 100 kPa.

When the thickness of the plate is 1/25 m, Kirchhoff-Love theory for thin plates is applicable. When the thickness is 1/10 m, the effect of shear through-the-thickness is significant and Mindlin's theory provides a better solution. The two configurations and the associated boundary conditions are shown in Figure 1.

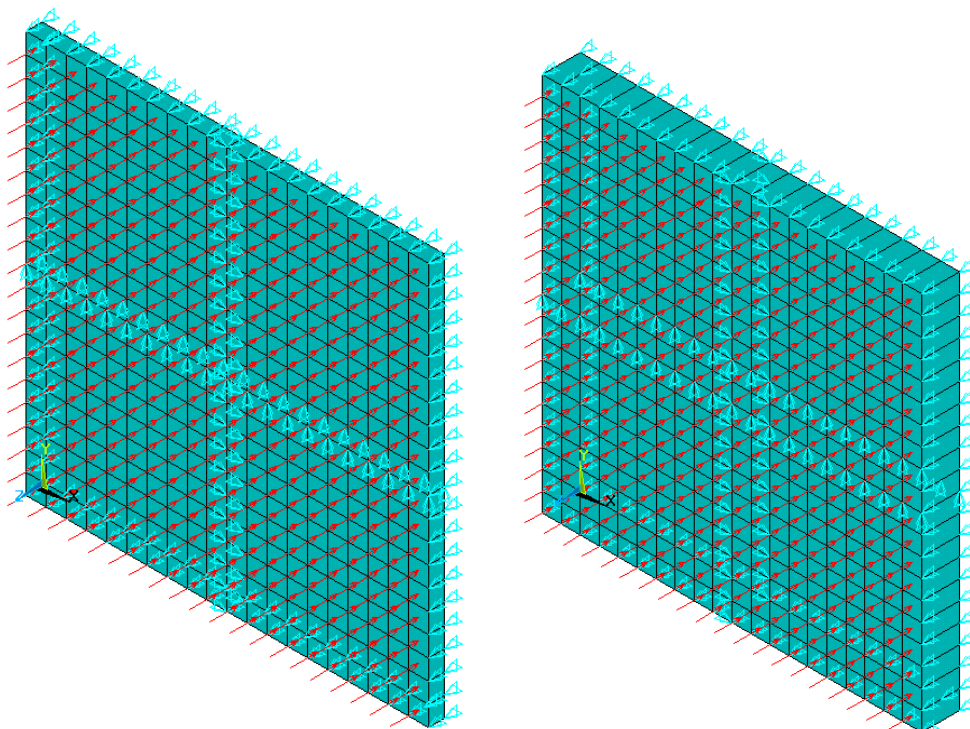**Figure 1** – *Simply supported isotropic plates under a uniform pressure load. The thin plate has a thickness of 1/25 m while the thick plate is 1/10 m thick.*

2.1 Exact solutions

For a thin rectangular plate of dimensions $a \times b \times h$, Young's modulus E, Poisson's ratio ν, simply supported along the four bottom edges and loaded uniformly on the top surface by a pressure q_0,

the exact solution for the displacement, $w(x, y)$, of the mid-surface is [1]

$$w(x, y) = \sum_{m=1}^{\infty} \sum_{n=1}^{\infty} \frac{16 q_0}{(2m-1)(2n-1)\pi^6 D} \times$$
$$\left[\frac{(2m-1)^2}{a^2} + \frac{(2n-1)^2}{b^2} \right]^{-2} \times \sin \frac{(2m-1)\pi x}{a} \sin \frac{(2n-1)\pi y}{b} \qquad (1)$$

where $D = h^3 E / (12(1 - \nu^2))$. The resultant moment in the x-direction is

$$M_{xx}(x, y) = -D \left(\frac{\partial^2 w}{\partial x^2} + \nu \frac{\partial^2 w}{\partial y^2} \right).$$

Plugging in the expression for $w(x, y)$, we get

$$M_{xx}(x, y) = \sum_{m=1}^{\infty} \sum_{n=1}^{\infty} \frac{16 q_0}{(2m-1)(2n-1)\pi^4} \left[\frac{(2m-1)^2}{a^2} + \nu \frac{(2n-1)^2}{b^2} \right] \times$$
$$\left[\frac{(2m-1)^2}{a^2} + \frac{(2n-1)^2}{b^2} \right]^{-2} \times \sin \frac{(2m-1)\pi x}{a} \sin \frac{(2n-1)\pi y}{b}. \qquad (2)$$

The bending stress in the plate is given by

$$\sigma_{xx}(x, y, z) = \frac{12 z}{h^3} M_{xx}(x, y). \qquad (3)$$

For a thick plate subjected to the same boundary conditions, the exact solution for the mid-plane displacement from Mindlin theory is [2, 3, 4]

$$w(x, y) = \sum_{m=1}^{\infty} \sum_{n=1}^{\infty} \frac{16 q_0}{(2m-1)(2n-1)\pi^6 D} \times$$
$$\left[\frac{(2m-1)^2}{a^2} + \frac{(2n-1)^2}{b^2} \right]^{-2} \times \sin \frac{(2m-1)\pi x}{a} \sin \frac{(2n-1)\pi y}{b} \times \qquad (4)$$
$$\left\{ 1 + \frac{\pi^2 h^2}{6 \varkappa (1-\nu)} \left[\frac{(2m-1)^2}{a^2} + \frac{(2n-1)^2}{b^2} \right] \right\}$$

The shear correction factor $\varkappa$ for a uniform cross-section is usually taken to be 5/6. We can find the resultant bending moment and shear force from the expression for $w(x, y)$ for a simply supported plate in a straightforward manner [4]. The expressions for these are

$$M_{xx}(x, y) = \sum_{m=1}^{\infty} \sum_{n=1}^{\infty} \frac{16 q_0}{(2m-1)(2n-1)\pi^4} \left[\frac{(2m-1)^2}{a^2} + \nu \frac{(2n-1)^2}{b^2} \right] \times$$
$$\left[\frac{(2m-1)^2}{a^2} + \frac{(2n-1)^2}{b^2} \right]^{-2} \times \sin \frac{(2m-1)\pi x}{a} \sin \frac{(2n-1)\pi y}{b}, \qquad (5)$$

and

$$Q_{zx}(x,y) = \sum_{m=1}^{\infty} \sum_{n=1}^{\infty} \frac{16q_0}{(2n-1)a\pi^3} \left[\frac{(2m-1)^2}{a^2} + \frac{(2n-1)^2}{b^2} \right] \times$$

$$\left[\frac{(2m-1)^2}{a^2} + \frac{(2n-1)^2}{b^2} \right]^{-2} \times \cos\frac{(2m-1)\pi x}{a} \sin\frac{(2n-1)\pi y}{b}, \tag{6}$$

The bending and transverse shear stresses in the plate are given by

$$\sigma_{xx}(x,y,z) = \frac{12z}{h^3} M_{xx}(x,y) \quad \text{and} \quad \sigma_{zx}(x,y,z) = \frac{1}{h\varkappa} Q_{zx}(x,y) \left(1 - \frac{4z^2}{h^2} \right). \tag{7}$$

2.2 The SHELL181 element

The SHELL181 element has 4 nodes with three translational and three rotational degrees of freedom at each node and linear interpolation is used within the element. Several options are available for the element of which the number of integration points through the thickness (specified using the SECDATA command) and the in-plane integration algorithm (KEYOPT(3)={0,2}) are of interest for an isotropic plate. Other options, including the number of layers and anisotropic material properties will be discussed later in the report.

The displacement w at the bottom of the thin plate (along the line $y = 0$) and the stresses σ_{xx} at the top and bottom surfaces of the plate (at $y = 0$) are shown in Figure 2 (p. 8). These quantities are compared with the exact solution directly and also in terms of a percent difference defined as

$$\text{Difference}(\%) = \frac{\text{ANSYS solution} - \text{Exact solution}}{\text{ANSYS solution}} \times 100.$$

The exact solution is shown by dashed lines. The solid lines are the simulated results. We can observe that effect of mesh refinement on the *displacement* solution in parts *a* and *b* of the figure. A well-converged solution is obtained for $n = 80$, i.e., when there are 80 elements along an edge of the plate. The ANSYS$^{\text{TM}}$ result differs from the exact solution by 4%-6%. The *stress* solution is shown in parts *c* and *d* of the figure. The solution converges for $n = 80$ but there are large errors at the edges of the plate where the ANSYS$^{\text{TM}}$ solution flattens out instead to reaching the zero stress condition.

The effect of increasing the number of through-thickness integration points and of changing the KEYOPT value can be seen in parts *e* and *f* of the figure. These plots are for the $n = 80$ case. The plots show that the effect of changing the number of integration points and the in-plane integration algorithm is negligible for a thin isotropic plate under uniform load.

Figure 3 (p. 9) shows plots of the displacement (w), bending stress (σ_{xx}), and transverse shear stress (σ_{zx}) for the thicker plate. Differences between ANSYS$^{\text{TM}}$ results and exact (Mindlin) solutions are also shown in the Figure. Parts *a* and *b* of the figure show the effect of mesh refinement (n) and the number of through-thickness integration points (i) on the *displacement* solution. The Kirchhoff-Love (K) solution is stiffer than the Mindlin (M) solution. However, the ANSYS$^{\text{TM}}$ solution shows a displacement that is approximately 10% greater than the exact solution, suggesting that a higher-order plate theory is probably more appropriate for a plate thickness of $h = a/10$. Increasing the number of integration points and mesh refinement does not appear to affect the solution significantly.

Parts *c* and *d* of the plot show the bending stresses along the top and bottom surfaces of the

thick plate (along $y = 0$). The ANSYS$^{\text{TM}}$ simulations predict a higher level of stress than Mindlin theory. The difference is of the order of 8% at the center of the plate and increases at the edges of the plate.

The transverse shear stresses are shown in parts e and f of the figure and the difference between the Mindlin and ANSYS$^{\text{TM}}$ solutions is of the order of 20% in this case. The effect of increased mesh refinement and number of integration points through-the-thickness is not significant in these plots.

These results show that the shell formulation used in the ANSYS$^{\text{TM}}$ SHELL181 element is slightly less stiff than predicted by Kirchhoff-Love theory. This is probably because change of thickness is allowed by the element. The increase in error in the predicted stress as the edge of the plate is approached suggests that care should be exercised when extracting forces close to the boundary of a SHELL181 plate from a finite element solution.

2.3 The SOLSH190 element

The SOLSH190 element has 8 nodes with three translational degrees of freedom at each node. Linear interpolation is used to determine the behavior of the element and the orientation of the normal to the mid-surface (also called the director) is determined from the two nodes on either side of the mid-surface. The number of integration points through the thickness can be specified using the SECDATA command. Note that identical displacement boundary conditions have to be applied to both the top and bottom nodes of the plate for a simply supported condition to be simulated. If displacement boundary conditions are applied only to the bottom of the plate, there is a significant amount of twist in the boundary directors leading to a deviation from Kirchhoff-Love theory.

From the point of view of geometric modeling, the most convenient use of this element is to use one element through the thickness of the plate. Since the SOLSH190 element allows layers with different properties to be defined, sandwich composites may, in principle, be modeled using one element with three layers through the thickness. Alternatively, three elements may be stacked through the thickness to achieve the same effect. In this section we explore both the effect of mesh refinement and that of using layers or distinct elements through the thickness.

The ANSYS$^{\text{TM}}$ solution for a thin plate using SOLSH190 elements is compared with the exact solution and the SHELL181 solution in Figure 4 (p. 11). Part a of the figure shows the displacement along $y = 0$. There is apparently effect of refinement or if we use three elements or one element with three layers. However, the percent difference in part b of the figure shows that there are differences between the various solutions. The SOLSH190 solution is reasonably converged when the plate has $n = 80$ elements along an edge and one element through-the-thickness. But this converged solution is stiffer than that predicted by SHELL181 elements. Small differences are observed when three elements ($e = 3$) are used through-the-thickness than when one element with three layers ($l = 3$) is used; the three layer solution is stiffer than the three element solution.

On the other hand, the bending stresses predicted by the SOLSH190 and SHELL181 elements are nearly identical as can be seen in parts c and d of the figure.

Parts e and f of the figure show the transverse shear stresses predicted by the SOLSH190 element and compared with the exact solution. In this case the three element through-thickness solution predicts higher stresses at the edges of the plate while the converged solutions ($n = 80$ and $n = 160$) for the one element/one layer case are nearly identical.

For the thick plate, the effect of mesh refinement, elements through-thickness, and number of layers on the ANSYS$^{\text{TM}}$ solution is shown in Figure 5 (p. 12). Part a of the figure shows that the response of the SOLSH190 element is between 6%-8% less stiff than suggested by Mindlin theory.
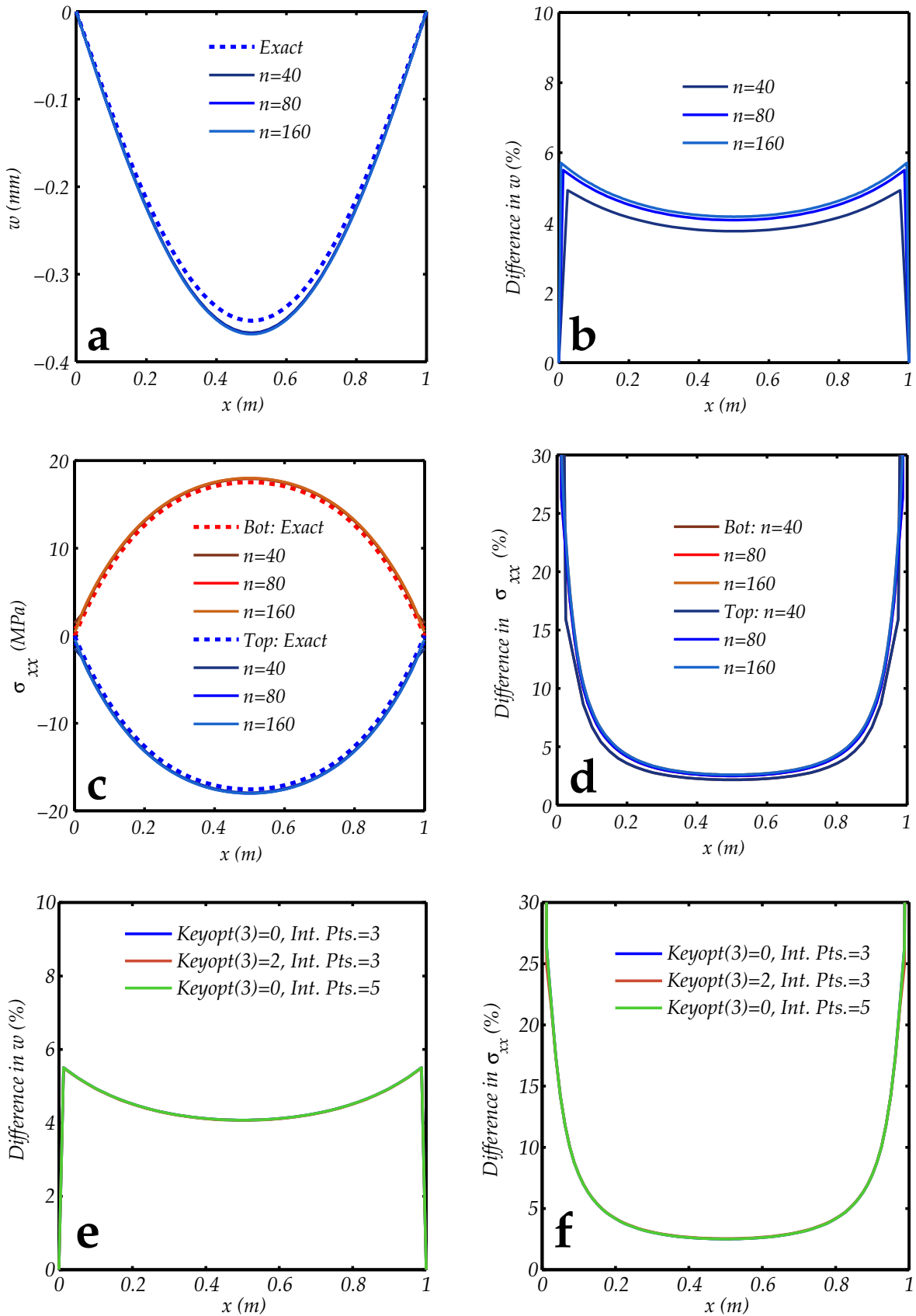
Figure 2 – *Effect of mesh refinement, KEYOPT values, and number of through-thickness integration points on solutions using SHELL181 elements for a thin simply supported plate under uniform pressure load.*
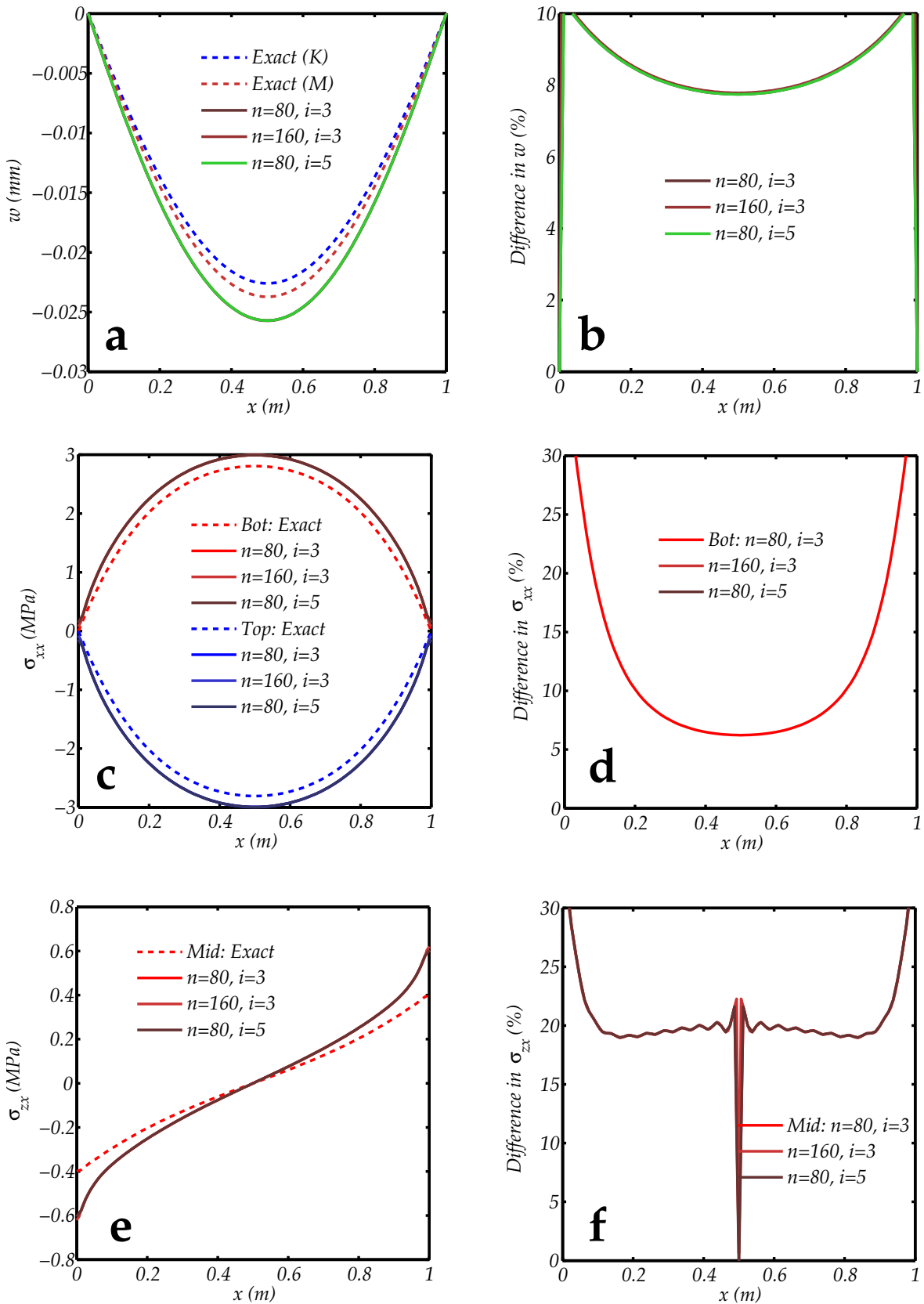
Figure 3 – *Displacements and stresses predicted by SHELL181 elements for a thick simply supported plate under uniform pressure load. The label $n = 80$ indicates that 80 elements were used along an edge. The label $i = 3$ indicates that three integration points were used through the thickness.*

Part b shows that the SOLSH190 element is, in general, stiffer than the SHELL181 element. If three elements are used through the thickness, the response is stiffer than when one element is used.

Parts c and d of the figure show the bending stress solutions. The bending stresses are higher than those predicted by Mindlin theory. Both SOLSH190 and SHELL181 elements predict nearly identical bending stresses. The errors at the boundary of the plate are lower when three elements are used through the thickness but higher at the center of the plate.

The mid-surface transverse shear stresses are shown in parts e and f of the figure. In this case the SHELL181 and three-element SOLSH190 results are quite close but differ significantly from Mindlin theory at the edges of the plate. There are slight differences between the other SOLSH190 solutions, but all options lead to values that are close to Mindlin theory at the boundaries and the center of the plate.

2.4   The SOLID185 element

The SOLID185 element is also a linear element with three translational degrees of freedom at each of its 8 nodes. This element is convenient for checking the performance of shell and solid shell elements for situations where exact solutions are not available. Simulations have shown that three elements through the thickness are adequate for modeling isotropic plates. Most of the results discussed in this section use three SOLID185 elements through the thickness of the plate. Stresses and displacements predicted by SOLID185 elements are compared with SHELL181 simulations (with KEYOPT(3) = 0, 3 integration points through-thickness, 80 elements along an edge) and SOLSH190 simulations (1 layer, 3 through-thickness integration points, 80 elements along edge).

Displacements and stresses for the simply supported thin plate under uniform pressure load are shown in Figure 6 (p. 13). The SOLID185 results include a mesh refinement study ($n = 40$, $n = 80$, $n = 160$) with KEYOPT(2) = 2 which is an enhanced strain formulation. The $n = 80$ case is also compared with the situation where KEYOPT(2)=0 when a full $\bar{B}$ integration is used. The effect of the number of elements though the thickness is examined by changing the number of elements through-thickness from 3 to 5 ($e = 5$).

Part a of the figure shows that when the full integration is used, the response of the plate is significant less stiff than that predicted by Kirchhoff-Love plate theory. The difference between the "exact" solution and the ANSYS$^{\text{TM}}$ results shown in part b indicates that the SOLID185 solution converges to the SOLSH190 solution with increasing mesh refinement. SHELL181 elements give a larger absolute displacement.

If we examine the bending stress solutions in parts c and d of the figure, we once again see that fully integrated SOLID185 elements underestimate the stress significantly. However, the difference between SOLID185, SOLSH190, and SHELL181 elements is marginal as far as the bending stress is concerned. Large errors are again observed at the edges of the plate because of a flattening of the stress distribution. This may only be an artifact of the interpolation process used by ANSYS$^{\text{TM}}$ to populate nodal stress data.

The mid-surface transverse shear stress results shown in parts e and f of the figure indicate that $\bar{B}$ and enhanced strain methods give nearly identical results that differ from Kirchhoff-Love theory at the edges of the plate. However, the SOLSH190 and SOLID185 results are quite different with the SOLSH190 simulations giving results closest to the exact solution.

For the thick plate, the effect of mesh refinement and integration points (through the thickness) on the ANSYS$^{\text{TM}}$ solution is shown in Figure 7 (p. 14). The results are similar to those for a thin plate except that an increase in the number of elements through-thickness ($e = 5$) gives a less stiff solution than SOLSH190 elements and three SOLID185 elements through the thickness.
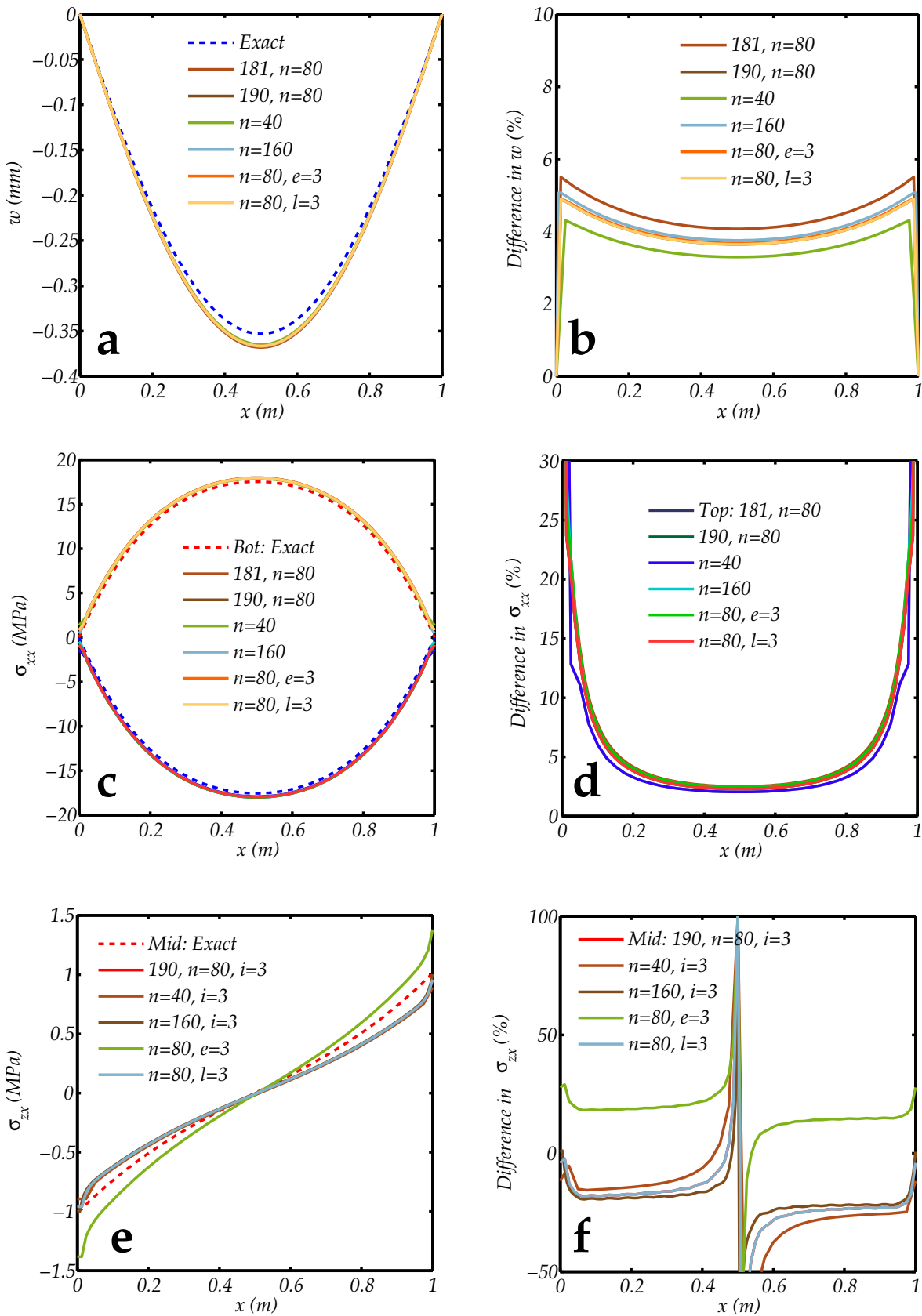
Figure 4 – *Displacement and stresses in a thin plate modeled with SOLSH190 elements under a uniform pressure load. The effect of mesh refinement, the number of elements through-thickness, and the number of layers in an elements can be observed from the plots.*
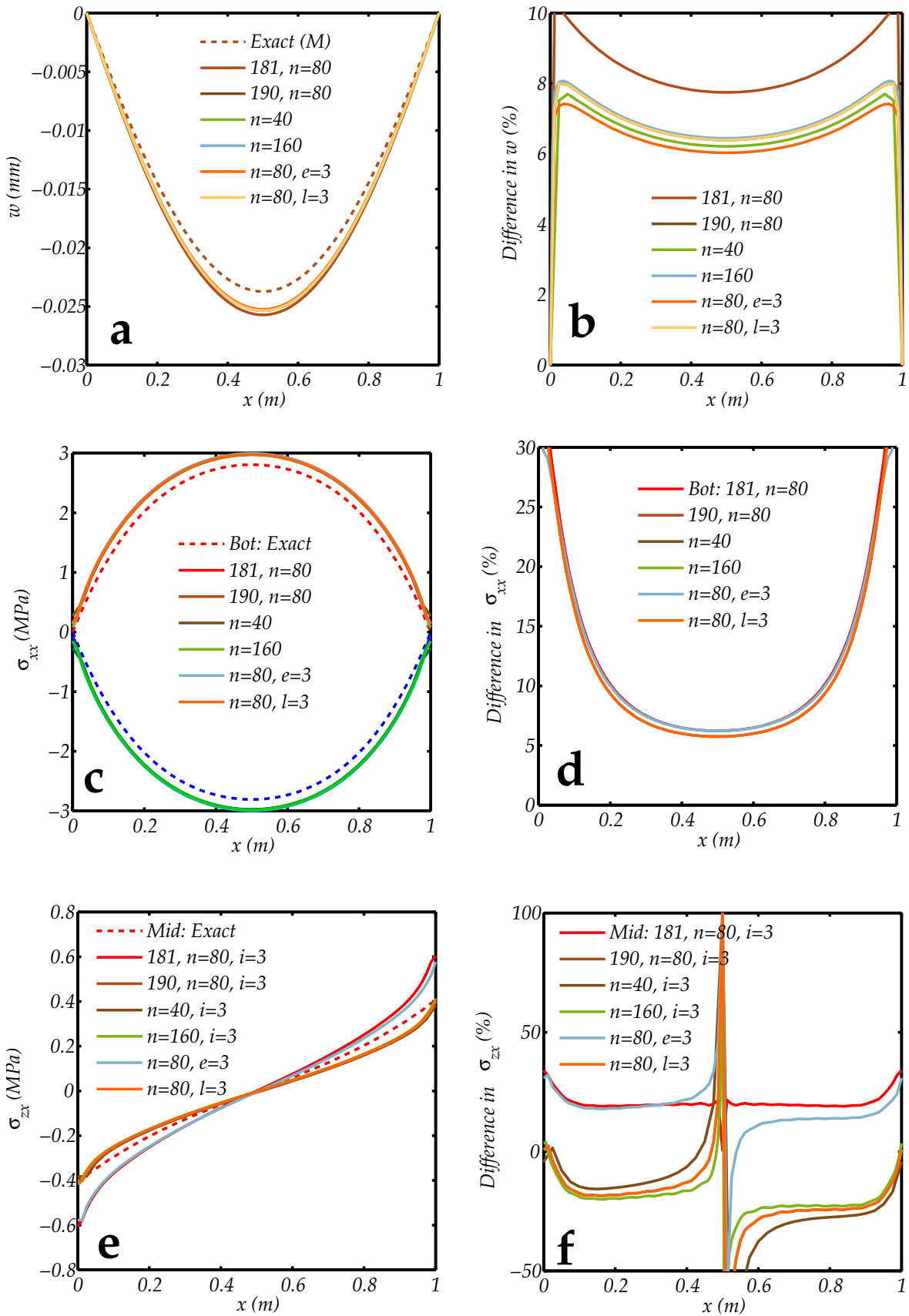
Figure 5 – *Thick plate solutions with SOLSH190 elements for a simply supported plate under uniform pressure load.*
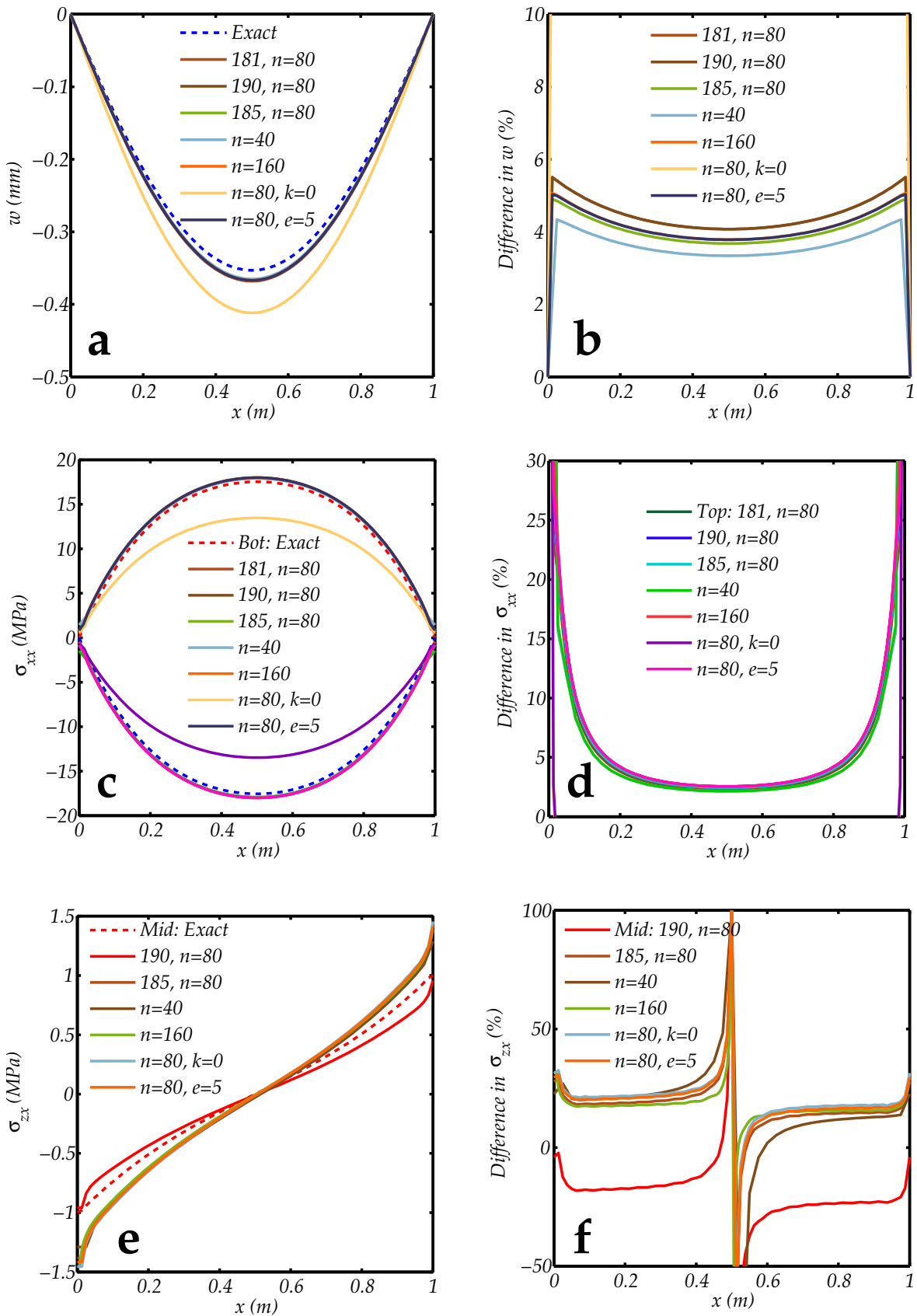
Figure 6 – *Comparison of stresses and displacements predicted by SOLID185 elements for a thin simply supported plate under uniform pressure load.*
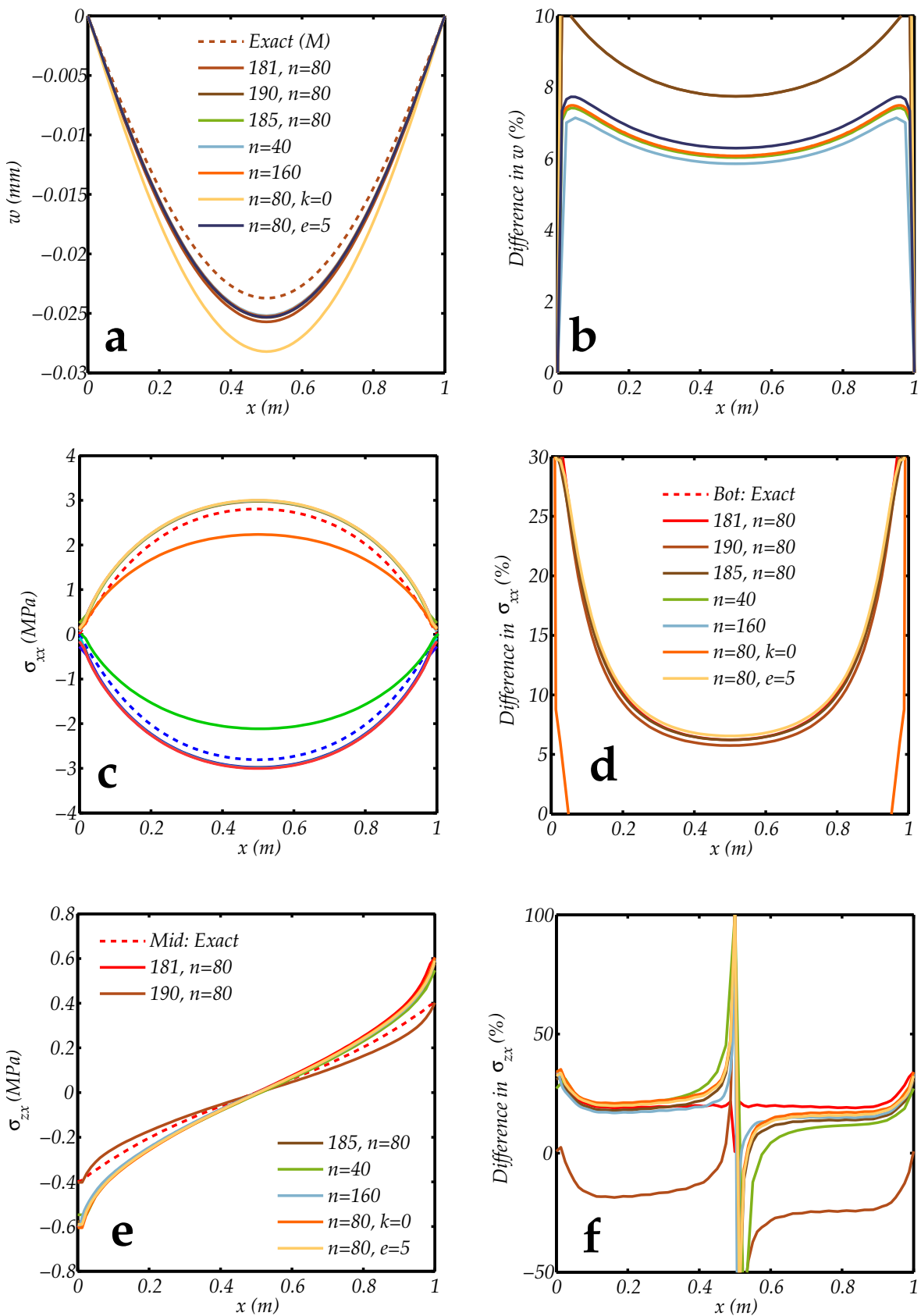
Figure 7 – *Solutions for a thick simply supported plate under uniform pressure load using SOLID185 elements.*

3   Isotropic plate loaded by boundary moments

Another problem for which analytical solutions are readily available is the situation where an isotropic plate is loaded by boundary moments. In this section we compare the analytical solution from Kirchhoff-Love theory with ANSYS$^{\text{TM}}$ solutions using SHELL181, SOLSH190, and SOLID185 elements. The plate is square (1 m long) and made of an isotropic material with Young's modulus 200 GPa and Poisson's ratio 0.27. The thickness of the plate is 1/25 m. The four edges of the plate are simply supported. The edges at $y = -b/2$ and $y = b/2$ are loaded with a boundary moment of 10 kN-m as shown in Figure 8.
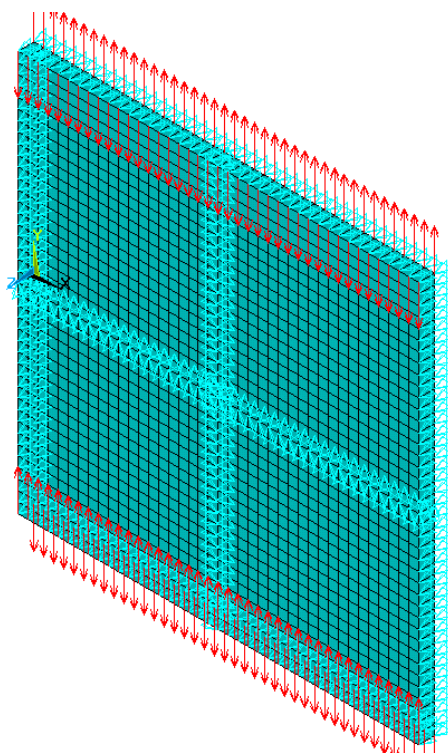

Figure 8 – Simply supported isotropic plate under uniform moment loads along two opposite edges.

3.1   Exact solutions

For a thin rectangular plate loaded by a uniform edge moment M_0, the exact solution for the transverse displacement is [1]

$$w(x,y) = \frac{2M_0 a^2}{\pi^3 D} \sum_{m=1}^{\infty} \frac{1}{(2m-1)^3 \cosh \alpha_m} \sin \frac{(2m-1)\pi x}{a} \times$$
$$\left[\alpha_m \tanh \alpha_m \cosh \frac{(2m-1)\pi y}{a} - \frac{(2m-1)\pi y}{a} \sinh \frac{(2m-1)\pi y}{a} \right]$$

where

$$\alpha_m = \frac{\pi(2m-1)b}{2a} \, .$$

The bending moment resultants are

$$M_{xx}(x,y) = \frac{2M_0(1-\nu)}{\pi} \sum_{m=1}^{\infty} \frac{1}{(2m-1)\cosh\alpha_m} \sin\frac{(2m-1)\pi x}{a} \left[-\frac{(2m-1)\pi y}{a} \sinh\frac{(2m-1)\pi y}{a} + \right.$$
$$\left. \left\{ \frac{2\nu}{1-\nu} + \alpha_m \tanh\alpha_m \right\} \cosh\frac{(2m-1)\pi y}{a} \right]$$

$$M_{yy}(x,y) = \frac{2M_0(1-\nu)}{\pi} \sum_{m=1}^{\infty} \frac{1}{(2m-1)\cosh\alpha_m} \sin\frac{(2m-1)\pi x}{a} \left[\frac{(2m-1)\pi y}{a} \sinh\frac{(2m-1)\pi y}{a} + \right.$$
$$\left. \left\{ \frac{2}{1-\nu} - \alpha_m \tanh\alpha_m \right\} \cosh\frac{(2m-1)\pi y}{a} \right]$$

and the shear force resultants are

$$Q_{zx}(x,y) = \frac{4M_0}{a} \sum_{m=1}^{\infty} \frac{1}{\cosh\alpha_m} \cos\frac{(2m-1)\pi x}{a} \cosh\frac{(2m-1)\pi y}{a}$$
$$Q_{yz}(x,y) = \frac{4M_0}{a} \sum_{m=1}^{\infty} \frac{1}{\cosh\alpha_m} \sin\frac{(2m-1)\pi x}{a} \sinh\frac{(2m-1)\pi y}{a}.$$

The stresses are

$$\sigma_{xx} = \frac{12z}{h^3} M_{xx}, \quad \sigma_{yy} = \frac{12z}{h^3} M_{yy}, \quad \sigma_{zx} = \frac{1}{\varkappa h} Q_{zx} \left(1 - \frac{4z^2}{h^2} \right) \quad \text{and} \quad \sigma_{yz} = \frac{1}{\varkappa h} Q_{yz} \left(1 - \frac{4z^2}{h^2} \right).$$

3.2 SHELL181 element

Figure 9 (p. 17) shows plots of the transverse displacement, the bottom-surface bending stress, and the mid-surface transverse shear stress in the plate along the line $x = a/2$. The results show that the solution converges with mesh refinement. However, convergence is slower than for the situation where a uniform pressure is applied to the plate. The error at the edge of the plate appears to increase with increased refinement. Most of the results are for the case where a single layer ($l = 1$) is used through the plate thickness. Results are identical when three layers ($l = 3$) of identical thickness are used instead.

The difference between the ANSYS$^{\text{TM}}$ solution and the exact results are less than 6% for the displacement (w) and the bending stress (σ_{yy}). However, as can be seen in parts e and f of the figure, there is a large difference between the ANSYS$^{\text{TM}}$ solution for the transverse shear stress (σ_{yz}) and that predicted by Kirchhoff-Love theory, even though the trend is similar.

3.3 SOLSH190 element

When SOLSH190 elements are used to model the plate, moments cannot be applied directly to the edges of the plate. Instead, forces of equal magnitude but opposite sign can be applied to the top and bottom edges of the plate when one element is used to model the thickness of the plate. Alternatively, a gradient surface force distribution of peak magnitude $6M_0/h^2$ and slope $12M_0/h^3$ can be applied to the edge areas (identified as $bc = 2$ in the plots).

Figure 10 (p. 19) shows plots of the transverse displacements, bending stresses, and transverse shear stresses for a plate modeled with SOLSH190 elements. In general, as shown in part a of the figure, the ANSYS$^{\text{TM}}$ displacements are larger than the predicted values from Kirchhoff-Love theory. From part b of the figure we can see that the displacements obtained using SOLSH190 elements
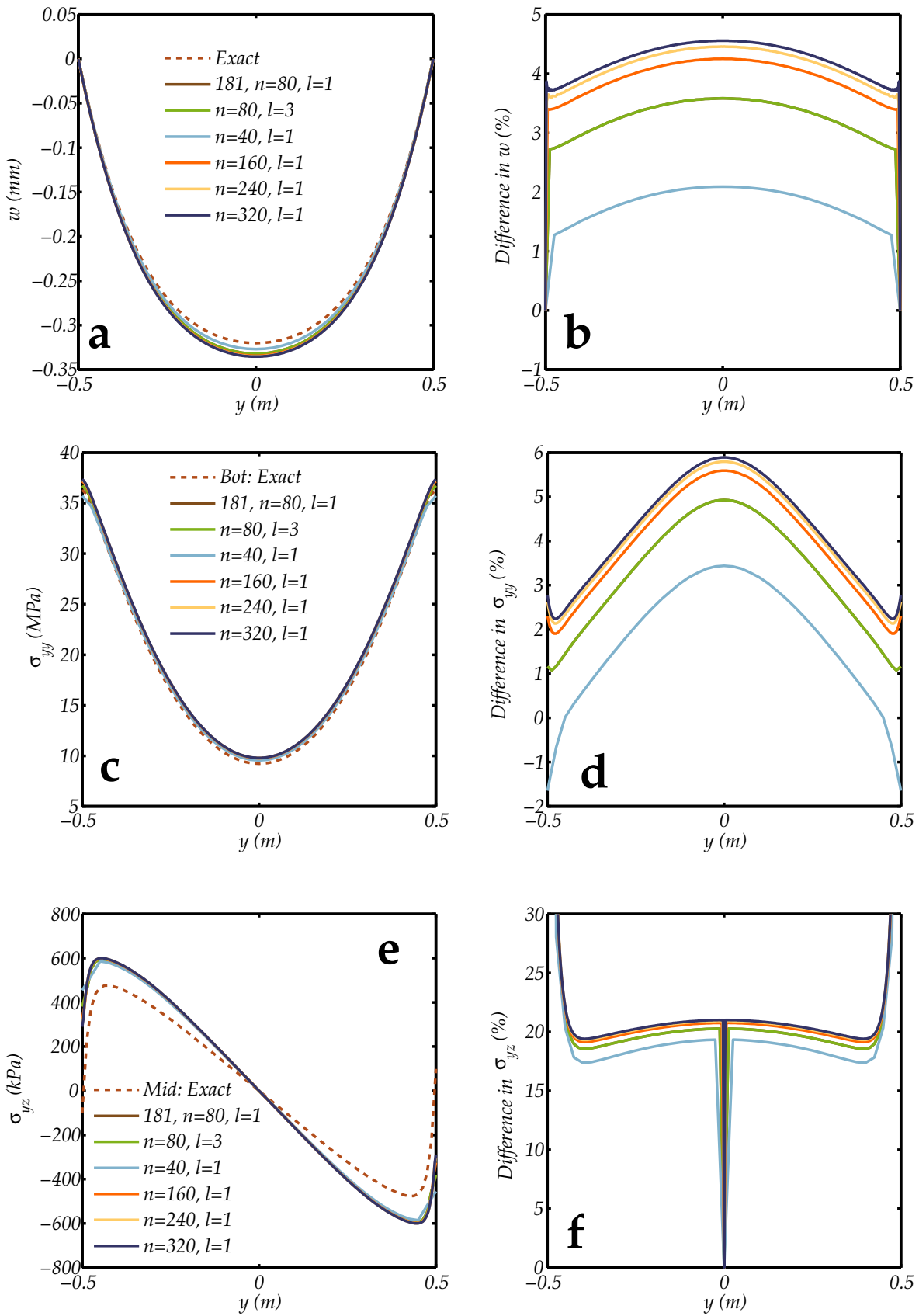
Figure 9 – *Effect of mesh refinement on displacement and stresses in a thin rectangular plate under a uniform moment load along the edges $y = \pm b/2$. The plate has been modelled with SHELL181 elements.*

are smaller than those predicted by SHELL181 elements (the difference is largest for SHELL181 elements). The SOLSH190 results converge rapidly beyond a mesh refinement of 160 elements per edge ($n = 160$) if a gradient surface force is applied along the edges ($bc = 2$). Instead, if forces are applied directly ($bc = 1$), the predicted displacements are significantly lower. The effect of the number of layers ($l = 1$ or $l = 3$) is negligible, but three elements through-thickness ($e = 3$) leads to a less stiff response and significant edge effects unless a gradient surface load is used to apply moments.

Part c of the figure indicates that the bending stresses predicted by ANSYS$^{\text{TM}}$ are lower than those given by Kirchhoff-Love theory. The smallest stresses are those using SHELL181 elements and the largest are from SOLSH190 elements with nodal force boundary conditions. The differences are largest at the center of the plate and smallest near the edges (see part d of the figure).

The transverse shear stresses (parts e and f of the figure) predicted by SHELL181 elements and SOLSH190 elements with three elements through-thickness are nearly identical and the percent difference is greater than zero for both these cases. However, for the single and three-layer SOLSH190 simulations, the shear stresses appear to be unaffected by the applied boundary conditions and these are always lower than the exact solution (in absolute value).
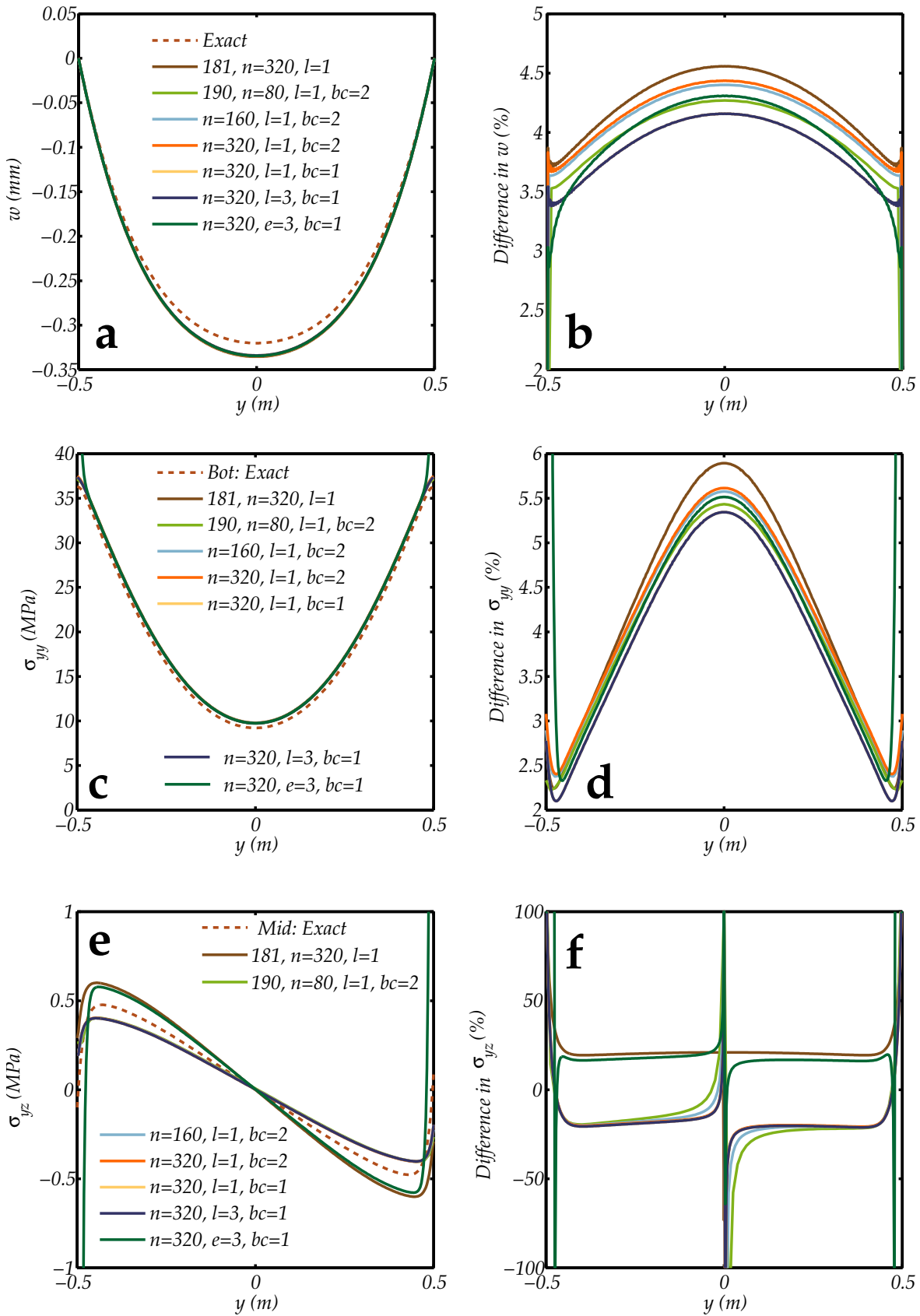
Figure 10 – *Effect of mesh refinement, number of elements through-thickness, and boundary conditions on the displacement and stresses in a thin rectangular plate under a uniform moment load along the edges $y = \pm b/2$. The plate has been modeled with SOLSH190 elements.*

4   Isotropic cantilever plate with concentrated edge load

Cantilevered plates are convenient for testing the behavior of finite elements because the results can be compared with beam bending solutions even though exact plate theory solutions for finite and short cantilevered plates may not be available because of corner singularities at the clamped end. In the simulations conducted for this section, a square plate of length 1 m, width 1 m, and thickness 1/25 m, made of an isotropic material with Young's modulus 200 GPa and Poisson's ratio 0.27, is clamped at one end and subjected to a linearly varying load at the free edge. The geometry and boundary conditions are shown in Figure 11. The applied load is 40.5 kN.
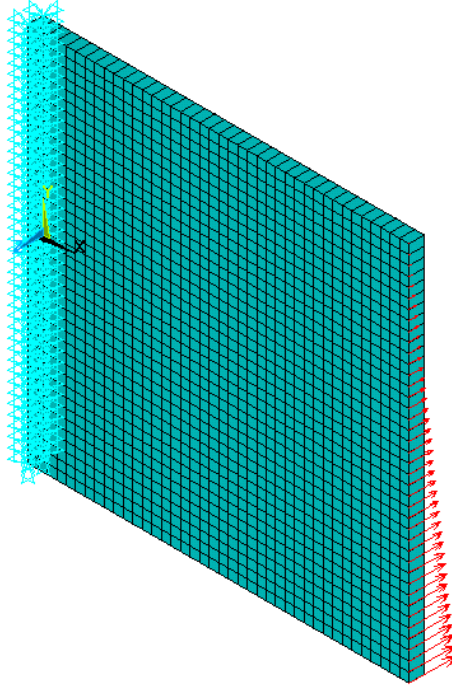

Figure 11 – *Cantilevered isotropic plate under distributed load along a free edge.*

4.1   Exact solution

In general, exact solutions for cantilever plates using plate theory are quite involved and very few solutions can be found in the literature. Reissner and Stein [5] provide a simplified theory for cantilever plates that is an improvement over the older Saint-Venant theory.

For a cantilever plate of dimensions $a \times b \times h$ with a concentrated end load $q_x(y)$ along $x = a$, the displacement is $w(x,y) = w_x(x) + y\theta_x(x)$ where

$$
\begin{aligned}
w_x(x) &= \frac{q_{x1}}{6bD}(3ax^2 - x^3) \\
\theta_x(x) &= \frac{q_{x2}}{2bD(1-v)}\left[x - \frac{1}{v_b}\left(\frac{\sinh(v_b a)}{\cosh[v_b(x-a)]} + \tanh[v_b(x-a)]\right)\right]
\end{aligned}
\tag{8}
$$

where $v_b = \sqrt{24(1-v)}/b$. If the applied load is a linear function of y, then

$$
q_{x1} = \int_{-b/2}^{b/2} q_0\left(\frac{1}{2} - \frac{y}{b}\right)\,\mathrm{d}y = \frac{bq_0}{2}\ ;\ \ q_{x2} = \int_{-b/2}^{b/2} yq_0\left(\frac{1}{2} - \frac{y}{b}\right)\,\mathrm{d}y = -\frac{b^2q_0}{12}\ .
$$

The resultant bending moments and shear forces are

$$
\begin{aligned}
M_{xx} &= -D\left(\frac{\partial^2 w}{\partial x^2} + \nu\,\frac{\partial^2 w}{\partial y^2}\right) \\
&= q_{x1}\left(\frac{x-a}{b}\right) - \left[\frac{3y\,q_{x2}}{b^3\,\nu_b\,\cosh^3[\nu_b(x-a)]}\right] \times \\
&\quad \left[6\sinh(\nu_b a) - \sinh[\nu_b(2x-a)] + \sinh[\nu_b(2x-3a)] + 8\sinh[\nu_b(x-a)]\right] \\
M_{xy} &= (1-\nu)D\,\frac{\partial^2 w}{\partial x\,\partial y} \\
&= \frac{q_{x2}}{2b}\left[1 - \frac{2 + \cosh[\nu_b(x-2a)] - \cosh[\nu_b x]}{2\cosh^2[\nu_b(x-a)]}\right] \\
Q_{zx} &= \frac{\partial M_{xx}}{\partial x} - \frac{\partial M_{xy}}{\partial y} \\
&= \frac{q_{x1}}{b} - \left(\frac{3y\,q_{x2}}{2b^3\,\cosh^4[\nu_b(x-a)]}\right) \times \left[32 + \cosh[\nu_b(3x-2a)] - \cosh[\nu_b(3x-4a)]\right. \\
&\quad \left. - 16\cosh[2\nu_b(x-a)] + 23\cosh[\nu_b(x-2a)] - 23\cosh(\nu_b x)\right].
\end{aligned} \tag{9}
$$

The stresses are

$$
\sigma_{xx} = \frac{12z}{h^3}\,M_{xx} \quad \text{and} \quad \sigma_{zx} = \frac{1}{\varkappa h}\,Q_{zx}\left(1 - \frac{4z^2}{h^2}\right).
$$

If the applied load at the edge is constant, we recover the solutions for a beam under a concentrated end load.

4.2   SHELL181 element

For a cantilever plate modeled with SHELL181 elements, the displacements and stresses along $y = 0$ are shown in Figure 12 (p. 22). Through the absolute difference in the displacement (between the exact and ANSYS$^{\text{TM}}$ solutions) is larger at the loaded edge of the plate, the relative difference is larger at the clamped edge. The effect of mesh refinement is small beyond a mesh consisting of 40 elements along an edge ($n = 40$). The effect of changing the in-plane integration algorithm (KEYOPT(3)) is also marginal. These differences increase as we move away from the center of the plate.

If we look at the bending stresses in parts c and d of the figure, we observe that the absolute difference in stress is larger at the clamped edge and falls to zero at the loaded edge. The jump in the value of the percent difference at the loaded edge is an artifact of division by a small number.

Reissner-Stein theory predicts a constant transverse shear stress along the mid-surface of the plate. However, as seen in parts e and f of the figure, the ANSYS$^{\text{TM}}$ predictions are more realistic. The difference between theory and simulation at the loaded edge is probably because of the way the load is averaged in the calculation of the "exact" solution.

4.3   SOLSH190 element

The displacements and stresses along $y = 0$ for the cantilever plate modeled with SOLSH190 elements are shown in Figure 13 (p. 24). Part a of the figure shows the displacements. The simulated displacements are between 5% to 10% lower than the theoretical value, with the largest relative discrepancy close to the clamped edge of the plate. The result produced by SHELL181 elements (KEYOPT(3)=0) cannot be distinguished from converged SOLSH190 solutions whether one layer
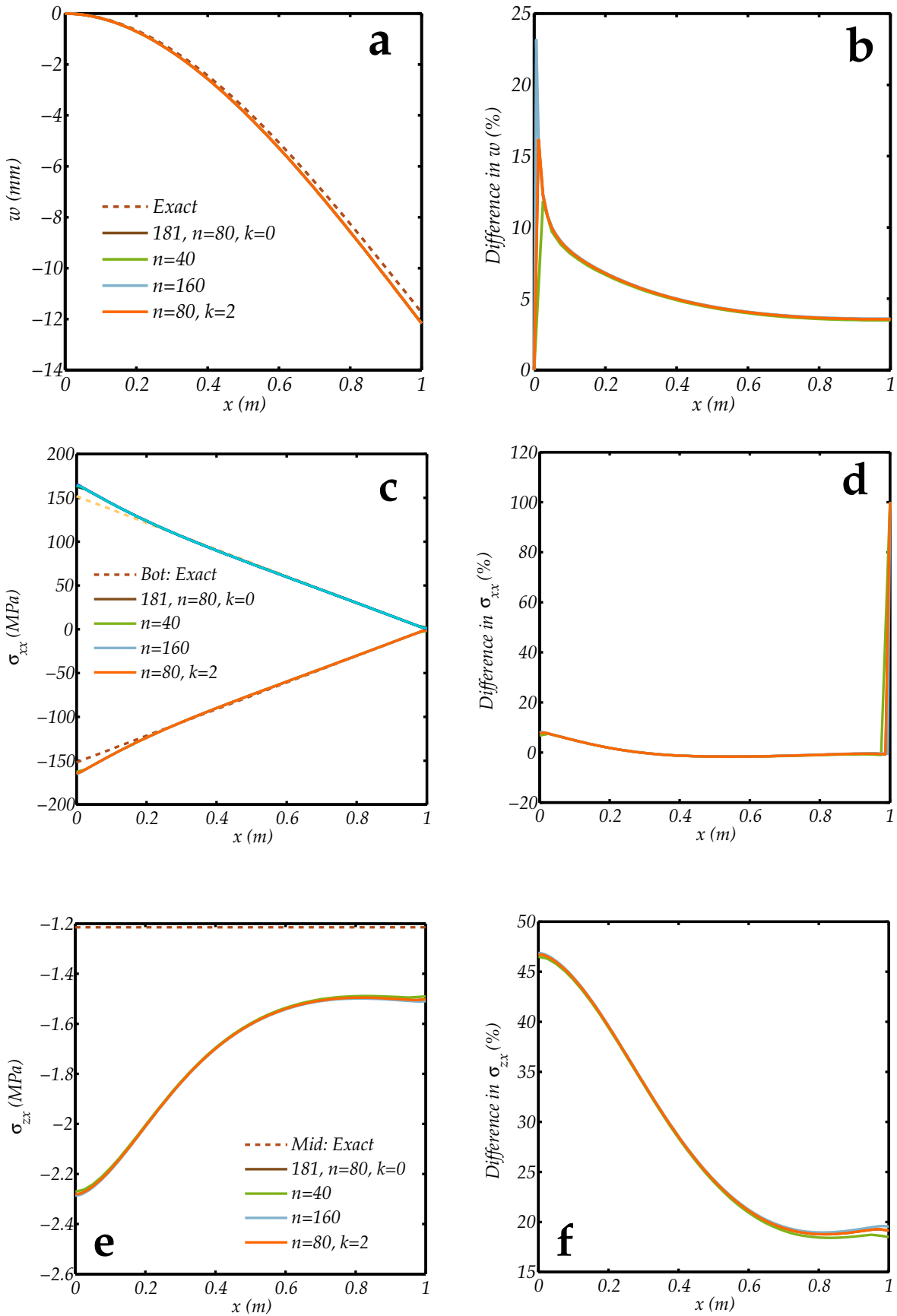
Figure 12 – *Effect of mesh refinement (n = 40, 80, 160) and KEYOPT(3) values*
(k = 0, k = 2) on the displacement and stresses along y = 0 in a thin
cantilever plate under a concentrated edge load.

($l = 1$) or three layers ($l = 3$) are used. Convergence occurs rapidly and a mesh with 40 elements to an edge ($n = 40$) gives results that are close to those for a mesh with 160 elements to an edge ($n = 160$).

Bending stresses predicted by ANSYS$^{\text{TM}}$ simulations are also nearly identical to the Reissner-Stein solution expect at the clamped end where the simulated results appear to be more accurate. The stresses along the bottom and top of the plate and the relative difference between ANSYS$^{\text{TM}}$ and theoretical results are shown in parts c and d of the figure, respectively. The difference is observed to be close to zero for all the cases explored.

However, as can be seen in parts e and f of the figure, the transverse shear stresses predicted by SHELL181 elements have significantly larger magnitudes (in absolute terms) than those predicted by SOLSH190 elements. The average shear stress along a cross-section ($y = 0$ in this case) from SOLSH190 elements is close to the value predicted by Reissner-Stein theory and appears to be more accurate.

4.4   SOLID185 element

Given that the Reissner-Stein theory does not appear to be very accurate, it is critical that the results from SHELL181 and SOLSH190 simulations be checked with full three-dimensional simulations with SOLID185 elements. There are several integration and element formulation options available for SOLID185 elements that can be accessed using KEYOPT(2). When this option is set to 0 ($k = 0$), the element is fully integrated and has the tendency to lock when used to model thin structures. The option 1 ($k = 1$) selects uniform reduced integration with hourglass control. Option 2 ($k = 2$) activates an enhanced strain formulation and option 3 ($k = 3$) is a simplified enhanced strain formulation. All these options have been explored and the results are shown in Figure 14 (p. 25). We have also explored the effect of mesh refinement in the plane of the plate ($n = 40, 80, 160$) and through the thickness ($e = 3, 5$, indicating the number of through-thickness elements). The SOLID185 results are compared with the Reissner-Stein solution and results using SHELL181 and SOLSH190 elements.

The outlier curve in part a of the figure corresponds to the case ($n = 80, k = 1$) where uniform reduced integration has been used. The response of the plate is excessively compliant when this option is used. All the other curves in the plot are nearly identical but lower than the Reissner-Stein solution as can be seen in part b of the figure. These results indicate that the three element types give us nearly identical values for the displacement.

Differences between various options become more obvious when we look at the bending stress curves in parts c and d of the figure. In this case we have two clear outliers, the cases $n = 80, k = 0$ and $n = 80, k = 1$. We have already discussed the $k = 1$ case which involves reduced integration. The $k = 0$ case involves full integration and predicted stresses that are lower than the Reissner-Stein estimate. All the other simulations give nearly identical results which are higher than those predicted by Reissner-Stein theory at the clamped edge. This indicates that the theoretical results are an underestimate of the actual stresses close to the clamped edge.

The error in the stresses predicted by fully integrated elements becomes clearer when we examine the transverse shear stresses in parts e and f of the figure. The difference between the SOLID185 prediction and the Reissner-Stein solution is of the order of 100% of the predicted value. Another new outlier appears in the results, shown by the light green line in part f. This case corresponds to the SOLSH190 calculation which is the closest to the theoretical value. However, all the other SOLID185 simulations indicate that the shear stress should be close to the value predicted by the SHELL181 elements. This suggests that the SOLSH190 elements is less accurate than SHELL181 elements when 1 layer/1 element is used through the thickness. Increasing the number of elements through the thickness ($e = 5$) tends to smooth out fluctuations at the boundaries.
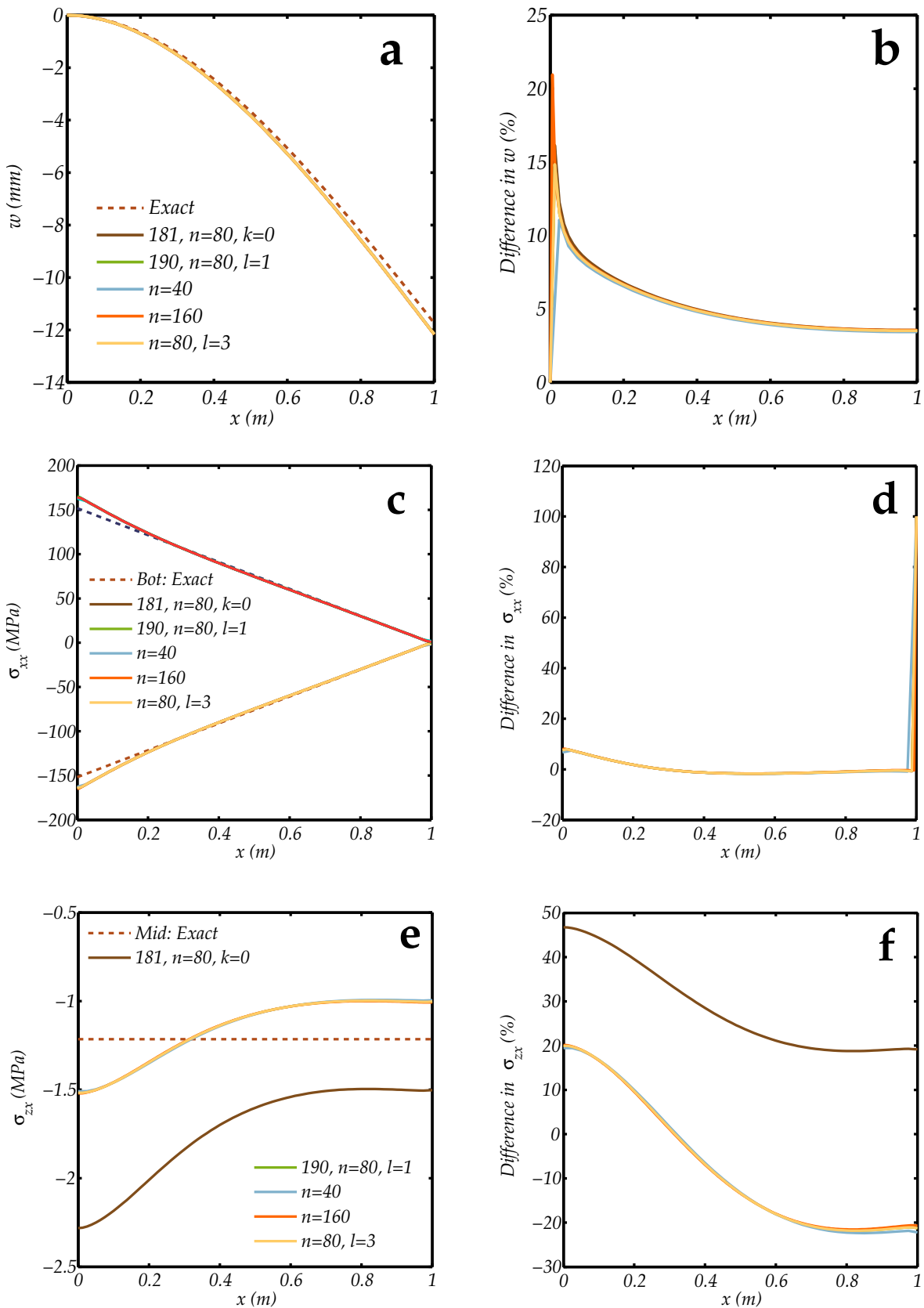
Figure 13 – *Effect of mesh refinement on displacement and stresses in a thin cantilever plate under concentrated edge load.*
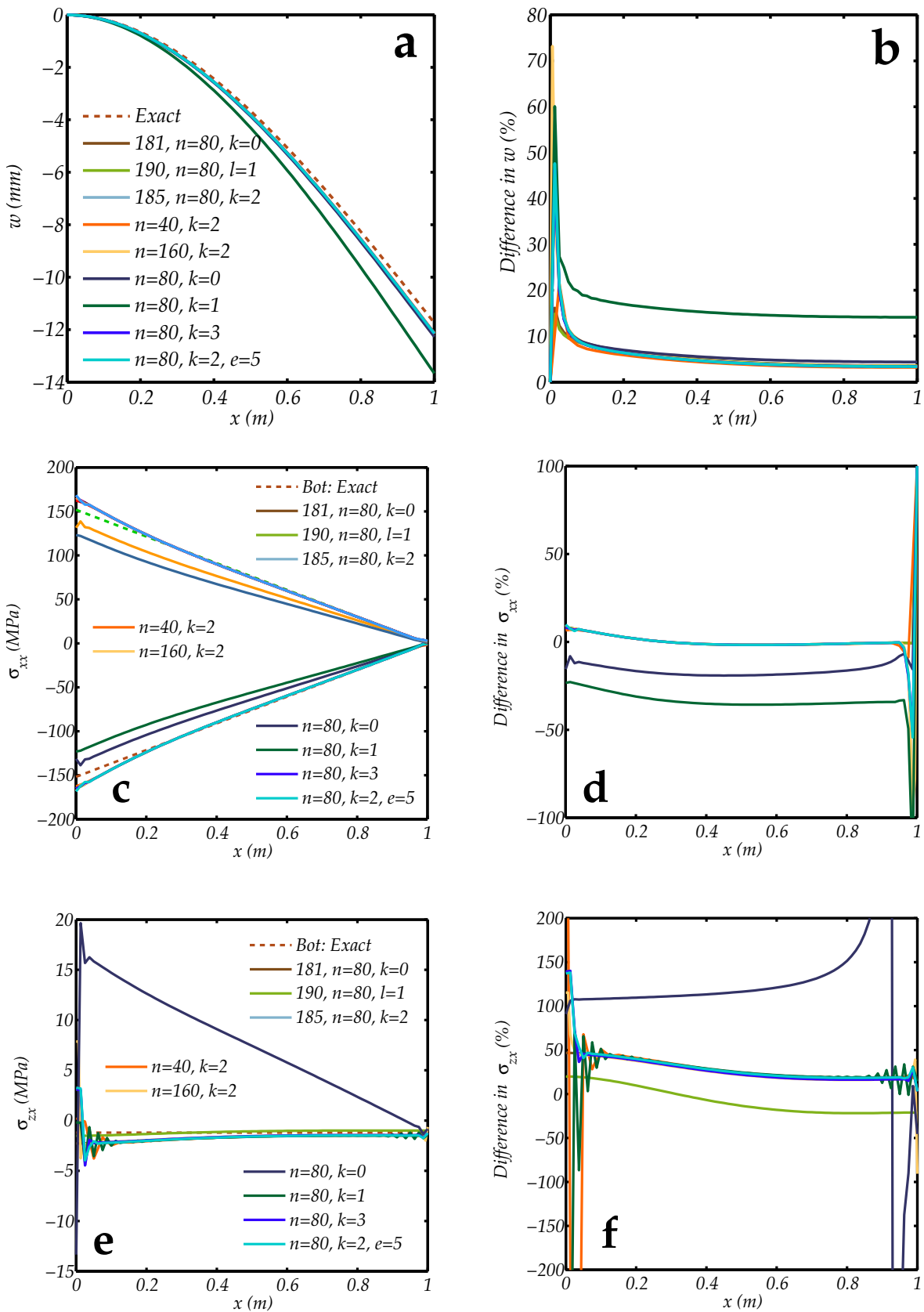
Figure 14 – *Effect of mesh refinement on displacement and stresses in a thin cantilever plate under concentrated edge load.*

5 Cantilever orthotropic plate with concentrated edge load

The simulations in the previous section showed that SHELL181 and SOLSH190 elements predicted slightly different stresses. In this section we examine whether these differences are magnified when the plate is thicker and made of an orthotropic material. The plate thickness is 1/10 m and the material properties are $E_{xx} = E_{yy} = 17.3$ GPa, $E_{zz} = 3.24$ GPa, $G_{xy} = 6.7$ GPa, $G_{yz} = G_{zx} = 1.2$ GPa, $\nu_{xz} = \nu_{yz} = 0.32$. The applied load is the same as in the previous section. A plot of the geometry and boundary conditions is shown in Figure 15. Since exact solutions for an orthotropic cantilevered plate are not available, comparisons have been made with the Reissner-Stein solutions for an isotropic plate with $E = 17.3$ GPa and $G = 6.7$ GPa. These solutions for an isotropic plate have been labelled "exact" in the plots that follow.
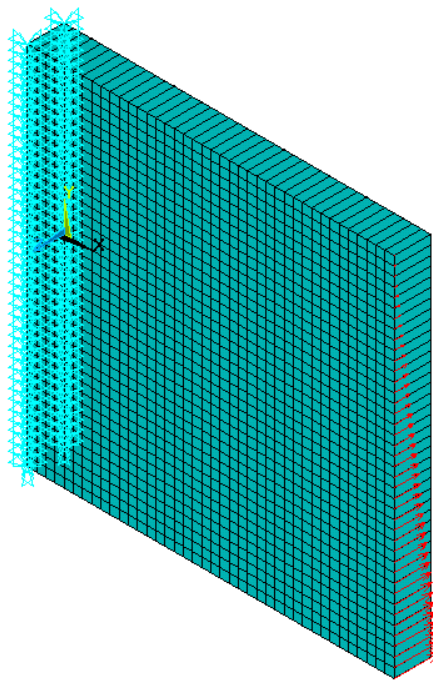

Figure 15 – Cantilevered orthotropic plate under distributed load along a free edge.

5.1 SHELL181 element

The displacements and stresses along $y = 0$ for the cantilever plate modeled with SHELL181 elements are shown in Figure 16 (p. 27). Convergence of the displacement solution is rapid as seen in parts *a* and *b* of the figure. The predicted displacements are larger than those for an isotropic plate, partly because rotation of the mid-surface normals due to shear has not been considered in the exact solution. No differences are observed when the options KEYOPT(3)=0 and KEYOPT(3)=2 are interchanged.

Interestingly, the bending stresses shown in parts *c* and *d* of the figure are remarkably close to that for an isotropic plate. A small discrepancy, similar to that observed in the previous section, can be seen at the clamped edge. The shear stress along $y = 0$ at the mid-surface is shown in parts *e* and *f* of the figure. Once again, there is a high shear stress at the clamped edge compared to the loaded edge. Also, convergence is slower close to the loaded edge compared to the clamped edge.
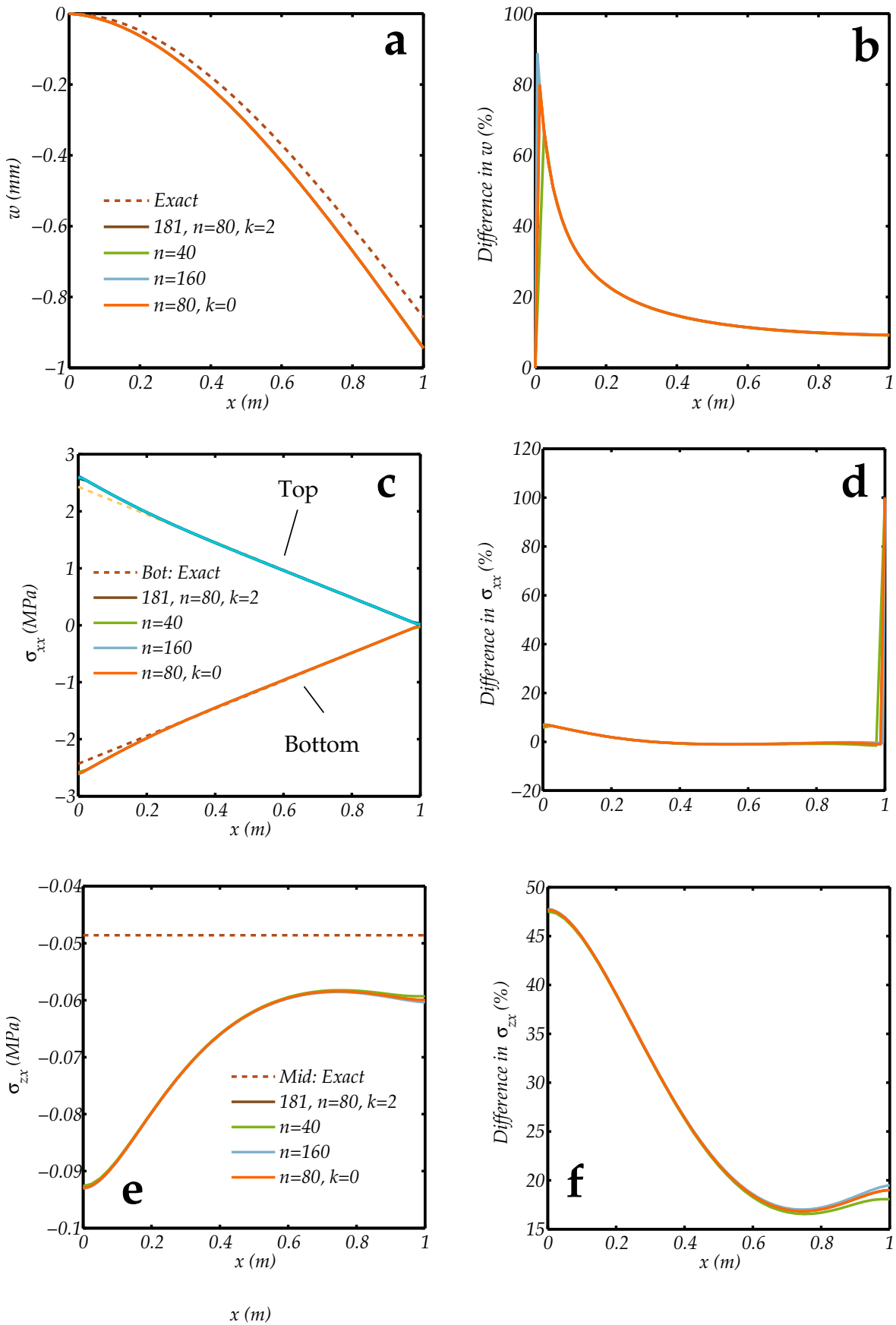
Figure 16 – *Effect of mesh refinement on displacement and stresses in a thick can-tilever plate under concentrated edge load.*

5.2 SOLSH190 element

Corresponding plots for simulations with SOLSH190 elements are shown in Figure 17 (p. 29). The displacements along $y = 0$ converge rapidly, are similar to those predicted by SHELL181 elements, and are not affected significantly whether one layer ($l = 1$), three layers ($l = 3$), or three elements are used ($e = 3$) through the thickness. The three-element solution is slightly more compliant than the one-element solution (with one or three layers).

Parts c and d of the figure show the bending stresses along $y = 0$ at the bottom and top of the plate. The SOLSH190 solutions are identical to the SHELL181 solutions except for the case where three elements are used through the thickness ($e = 3$). For that case, there is a significant amount of asymmetry at the loaded edge of the plate between the stresses at the top and bottom of the plate. The stresses at the clamped edge also diverge slightly from the SHELL181 solution and the one-element SHELL190 solutions. The reason for the difference appears to be the boundary conditions that have been applied to the model. At the clamped edge, all degrees of freedom have been suppressed at all the nodes while the load is applied only to nodes at the top of the plate along the loaded edge. These conditions are not identical to those assumed internally by ANSYS$^{\text{TM}}$ for SHELL181 elements and one-element SOLSH190 elements.

The transverse shear stress plots in parts e and f of the figure show some interesting behaviors. The SOLSH190 simulations with one element through the thickness predict lower shear stresses than SHELL181 simulations. However, when three SOLSH190 elements are use through the thickness, the stresses are quite close to those predicted by SHELL181 elements; except at the clamped and loaded edges. The discrepancies at the edges are due to the applied boundary conditions. This result strongly suggests that a single SOLSH190 element through the thickness may not produce accurate results. Comparisons with SOLID185 element in the next section further confirms this conjecture.

5.3 SOLID185 element

For a plate modeled with SOLID185 elements, the displacements and stresses along $y = 0$ are plotted in Figure 18 (p. 31). Predictions using SOLID185 elements are compared with the isotropic, "exact", solution, SHELL181 simulations with KEYOPT(3)=0, and one-element ($l = 1$) and three-element ($e = 3$) SOLSH190 calculations. The integration schemes considered for the SOLID185 element are uniform reduced integration ($k = 1$) and enhanced assumed strain ($k = 2$). Three through-thickness elements have been used in all the SOLID185 simulations.

The displacement plots in parts a and b of the figure show that convergence of the solution along $y = 0$ is rapid and is achieved with only 40 elements along an edge ($n = 40$). The outlier in green corresponds to a reduced integration calculation with SOLID185 elements. The light green outlier that becomes apparent in part b of the figure corresponds to a SOLSH190 calculation with one element through the thickness. A slightly smaller displacement is predicted by the ANSYS$^{\text{TM}}$ model when this options is used.

Parts c and d of the figure show the bending stresses at the top and bottom of the plate along $y = 0$. We find that the one-element SOLSH190 simulation and the SHELL181 simulation give nearly identical results. On the other hand, the three-element SOLSH190 simulation gives results that are similar to those using SOLID185 elements. The increase in the number of degrees of freedom and the resulting change in the nodal boundary conditions is responsible for the lack of symmetry between the top and bottom stresses when more than one element is used through the thickness.

Examination of the transverse shear stress plots in parts e and f of the figure shows that reduced integration of SOLID185 elements leads to fluctuations close to the boundaries. However, all the
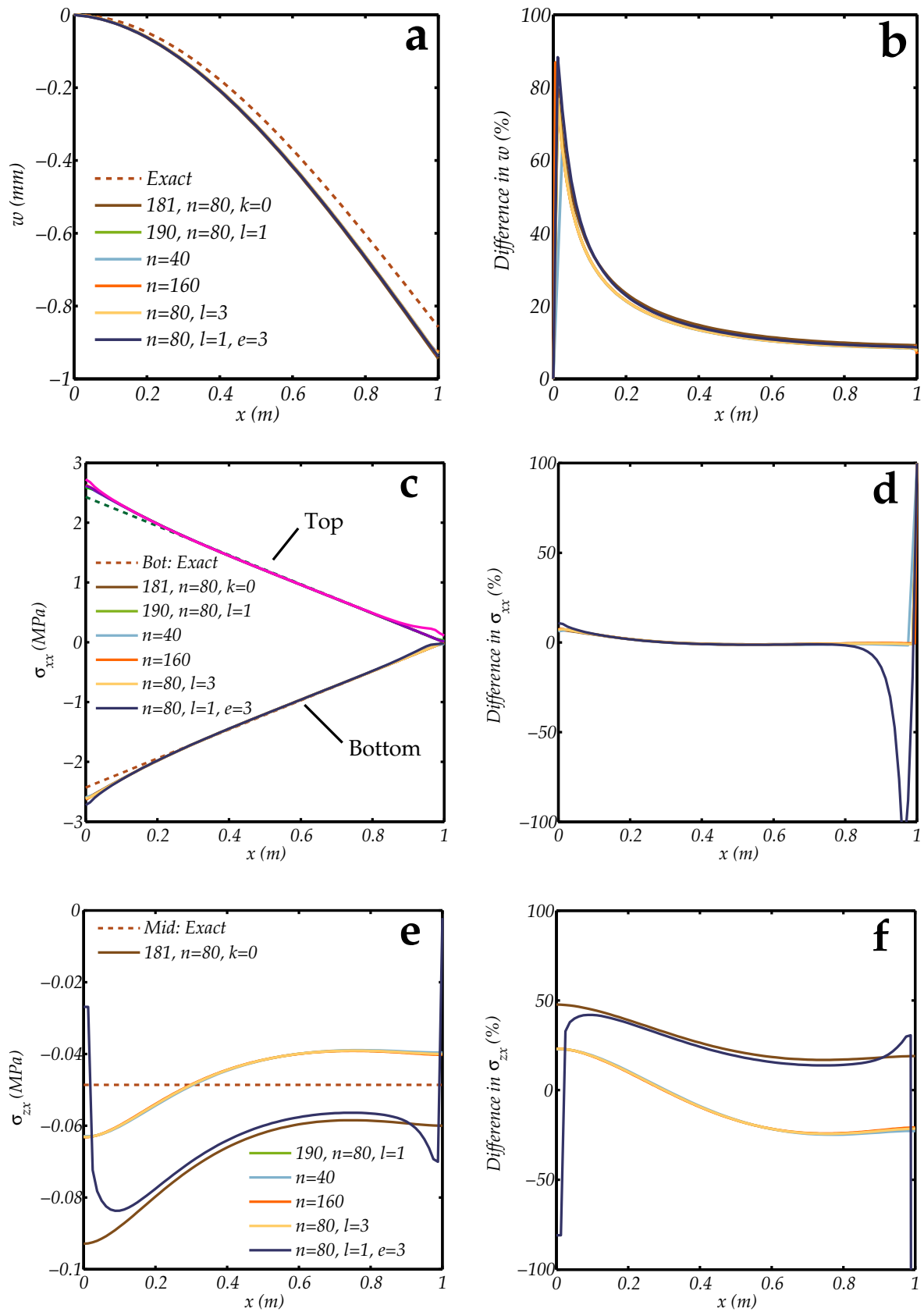
Figure 17 – *Effect of mesh refinement on displacement and stresses in a thick can-tilever plate under concentrated edge load.*

SOLID185 simulations produce results that are close to those predicted by SHELL181 elements and nearly identical to those produced by SOLSH190 elements with three through-thickness elements. This indicates that SOLSH190 elements with one through-thickness element are not very accurate in predicting transverse shear stresses.
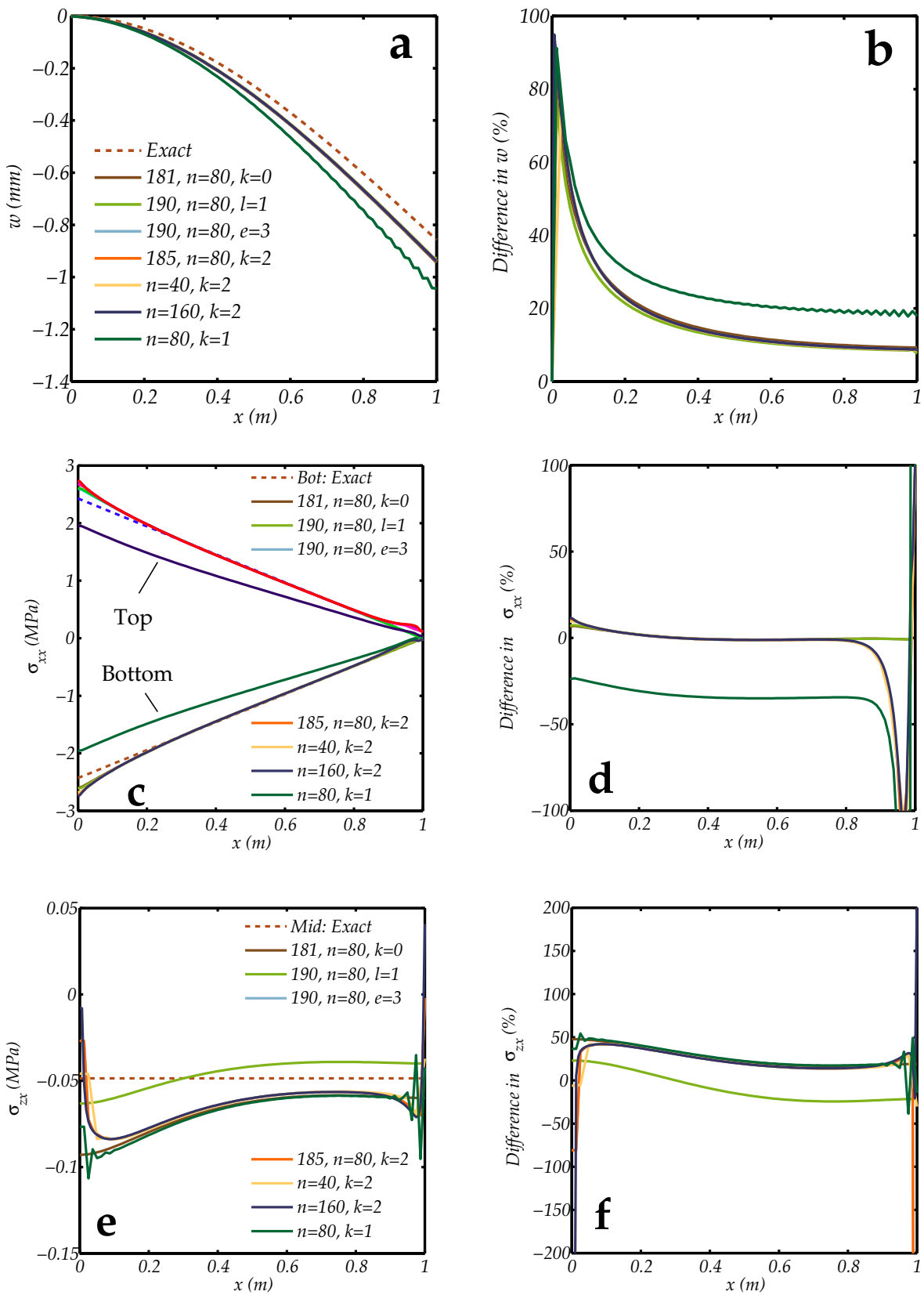
Figure 18 – *Effect of mesh refinement on displacement and stresses in a thick cantilever plate under concentrated edge load.*

6   Cantilevered isotropic sandwich plate with concentrated edge load

So far we have not truly explored the layering capabilities of ANSYS$^{\text{TM}}$ shell elements except to verify that layering commands had been correctly input into simulations and the correct data were being extracted. In this section we investigate true sandwich composites with significantly different facesheet/core geometries and material properties.

The sandwich panels have the same planar dimensions as before, 1 m × 1 m. Two sandwich panel models of different layer thicknesses are explored in this section:

1. a thin panel with facesheet thickness 1/1000th the panel length (i.e., 1 mm) and core thickness 1/50th the panel length (i.e., 20 mm), and

2. a thick panel with facesheet thickness 1/100th the panel length (i.e., 1 cm) and core thickness 1/10th the panel length (i.e., 10 cm).

The total applied load is 405 N, distributed linearly over the free edge as shown in Figure 19. The facesheets have moduli $E_f = 17.3$ GPa and $G_f = 6.7$ GPa. The core has moduli $E_c = 0.34$ MPa and $G_c = 0.11$ MPa.
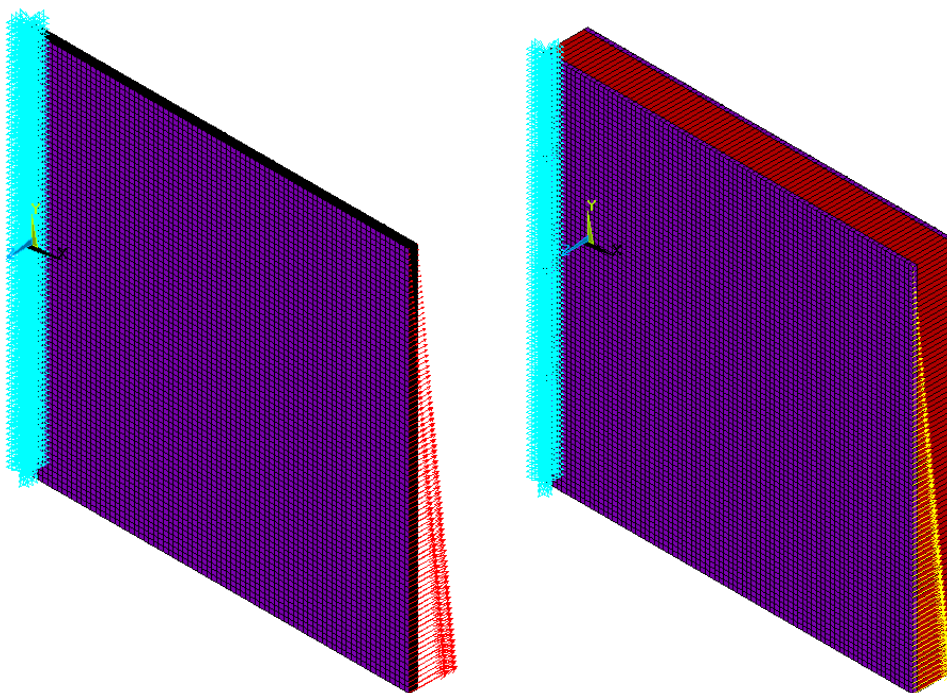

Figure 19 – *Models of isotropic sandwich plates under concentrated edge load.*

6.1   Exact solution

An exact solution that is valid at all points on a rectangular sandwich cantilevered plate is difficult to obtain because of the singularities at the clamped corners of the plate. However, an estimate of the deformation and stress along the center line can be obtained using classical sandwich beam

theory. Following Zenkert [6] (p. 63), the solution for "thin" facesheets is $w = w_b + w_s$ where

$$
\begin{aligned}
w_b(x) &= \frac{qa^3}{6D} \left(\frac{x}{a}\right)^2 \left(3 - \frac{x}{a}\right) \\
w_s(x) &= -\frac{D}{S} \frac{d^3 w_b}{dx^3} = \frac{qx}{S}
\end{aligned}
\tag{10}
$$

and the bending and shear contributions to the out-of-plane displacement, respectively. In the above equations, q is the applied load, D is the bending stiffness of the beam, S is the shear stiffness of the beam, and a is the length of the beam. For a linearly distributed edge load along the edge $x = a$, with maximum q_0 at $y = -b/2$ and minimum 0 at $y = b/2$, we have $q = bq_0/2$ where b is the width of the plate. The bending and shear stiffnesses are defined as

$$
D = \frac{f h^2 E_f}{2} \quad \text{and} \quad S = \frac{\varkappa h^2 G_c}{c}
$$

where E_f is the Young's modulus of the facesheets, G_c is the shear modulus of the core, c is the thickness of the core, and $h = f + c$ where f is the thickness of the facesheet. It is assumed that both facesheets have the same thickness.

The stresses are given by

$$
\begin{aligned}
\sigma_{xx} &= -E_f z \frac{d^2 w_b}{dx^2} = \frac{zqE_f}{D}(x - a) \\
\sigma_{zx} &= \frac{h G_c}{c} \frac{dw_s}{dx} = \frac{hqG_c}{cS}
\end{aligned}
\tag{11}
$$

where σ_{xx} is the bending stress in the facesheets, and σ_{zx} is the shear stress in the core.

For a sandwich beam with "thick" facesheets, the solution has the form [7] (p. 13)

$$
\begin{aligned}
w_b(x) &= \frac{qa^3}{6D} \left(\frac{x}{a}\right)^2 \left(3 - \frac{x}{a}\right) - \frac{2qD_f}{DS}[x - f(x)] \\
w_s(x) &= \frac{qx}{S} + \left(\frac{q}{S + 2S_f} - \frac{q}{S}\right) f(x)
\end{aligned}
\tag{12}
$$

where D_f and S_f are the bending and shear stiffnesses of the facesheets, defined as

$$
D_f = \frac{f^3 E_f}{12} \quad \text{and} \quad S_f = \varkappa f G_f
$$

where G_f is the shear modulus of the beam, and

$$
f(x) = \frac{1}{\alpha}\left[\sinh(\alpha x) + \{1 - \cosh(\alpha x)\}\tanh(\alpha a)\right], \quad \alpha = \left[\frac{SS_f}{(S + 2S_f)D_f}\right]^{1/2}.
$$

The corresponding stresses are

$$
\begin{aligned}
\sigma_{xx} &= \frac{zqE_f}{D}\left[(x - a) - \frac{2\alpha D_f}{S} \frac{\sinh[\alpha(x - a)]}{\cosh(\alpha a)}\right] - \frac{z_f q E_f}{S} \frac{2\alpha S_f}{S + 2S_f} \frac{\sinh[\alpha(x - a)]}{\cosh(\alpha a)} \\
\sigma_{zx} &= \frac{hqG_c}{cS}\left[1 - \frac{2S_f}{S + 2S_f} \frac{\cosh[\alpha(x - a)]}{\cosh(\alpha a)}\right]
\end{aligned}
\tag{13}
$$

where

$$z_f = \begin{cases} z - 1/2(c+f) & \text{for } z > 0 \\ z + 1/2(c+f) & \text{for } z < 0 \end{cases}.$$

6.2 SHELL181 element

The SHELL181 element appears to behave like a thin shell and produces results that match the thin-facesheet approximation for a sandwich beam. This can be seen from Figure 20 (p. 35). The figure shows displacements and stresses for the thin sandwich panel and compares those with the *thin-facesheet solution* discussed above. Parts *a* and *b* of the figure indicate that the thin-facesheet displacement along $y = 0$ is matched quite accurately except for a small discrepancy at the loaded edge. The bending stresses in parts *c* and *d* of the figure also show excellent agreement with the thin-facesheet approximation. The transverse shear stresses shown in parts *e* and *f* of the figure are different from the thin-facesheet solution. However, the relative difference is less that ± 2 %.

An equivalent set of comparisons with the *thick-facesheet solution* are shown in Figure 21 (p. 36). From parts *a* and *b* of the figure we notice that the displacement predicted by SHELL181 elements is more than the exact, thick-facesheet, value. The effect of clamping is also more obvious in the exact solution in the form of a zero slope at the clamped end. The exact bending stresses at the clamped end are significantly larger than the SHELL181 solution as seen in parts *c* and *d* of the figure. A similar effect is seen in the plots of the transverse shear stress in parts *e* and *f*, the exact stress near the clamped edge is considerably lower than the SHELL181 prediction. Since the thick-facesheet solution is more accurate, particularly in the region close to the clamped edge, we conclude that the solution generated by the SHELL181 element is not very accurate in this region of the plate when the layers are isotropic.

SHELL181 elements appear to predict reasonable results for the most part for the thin plate that is 22 mm thick (20 mm core + two 1 mm thick facesheets). However, the results are less satisfactory when we use these elements to model a shell that is 12 cm thick (10 cm core + two 1 cm facesheets). Note that the thickness of the sandwich plate is still of the order of 1/10th the planar dimensions, and, in principle, plate theory can be applied.

For the thick panel, SHELL181 elements continue to predict results that are close to the thin-facesheet solution as shown in Figure 22 (p. 37). But the thin facesheet solution is grossly inaccurate for a thick plate. The more accurate thick-facesheet solution is plotted with dashed lines in Figure 23 (p. 38). Clearly, there is a large discrepancy between the SHELL181 prediction and the thick-facesheet solution and the indication is that SHELL181 elements are grossly inaccurate when modeling thick sandwich panels.

Let us now look more closely at the results in Figure 22 (p. 37). Parts *a* and *b* of the figure show the displacements along $y = 0$, the center of the plate. We observe that convergence at the loaded edge is slow and the displacement converges to the thin-facesheet approximation for cantilever sandwich beams. The bending stresses in parts *c* and *d* of the figure also show that SHELL181 elements are predicting values that are close to the thin-facesheet approximation though convergence is faster. The transverse shear stresses in parts *e* and *f* of the figure also show a slow convergence to a value that is close to the thin-facesheet approximation.

On the other hand if we compare the same SHELL181 results with the thick-facesheet solution (see Figure 23, p. 38), the exact solution differs from the displacements predicted by ANSYS$^{\text{TM}}$ by more than 50%. The bending stresses differ by almost a factor of 10 and the transverse shear stresses are off by between 20% to 100%.

Comparisons of these results with SOLSH190 and SOLID185 simulations confirm the inaccuracy of the SHELL181 results. These comparisons are discussed in the following sections.
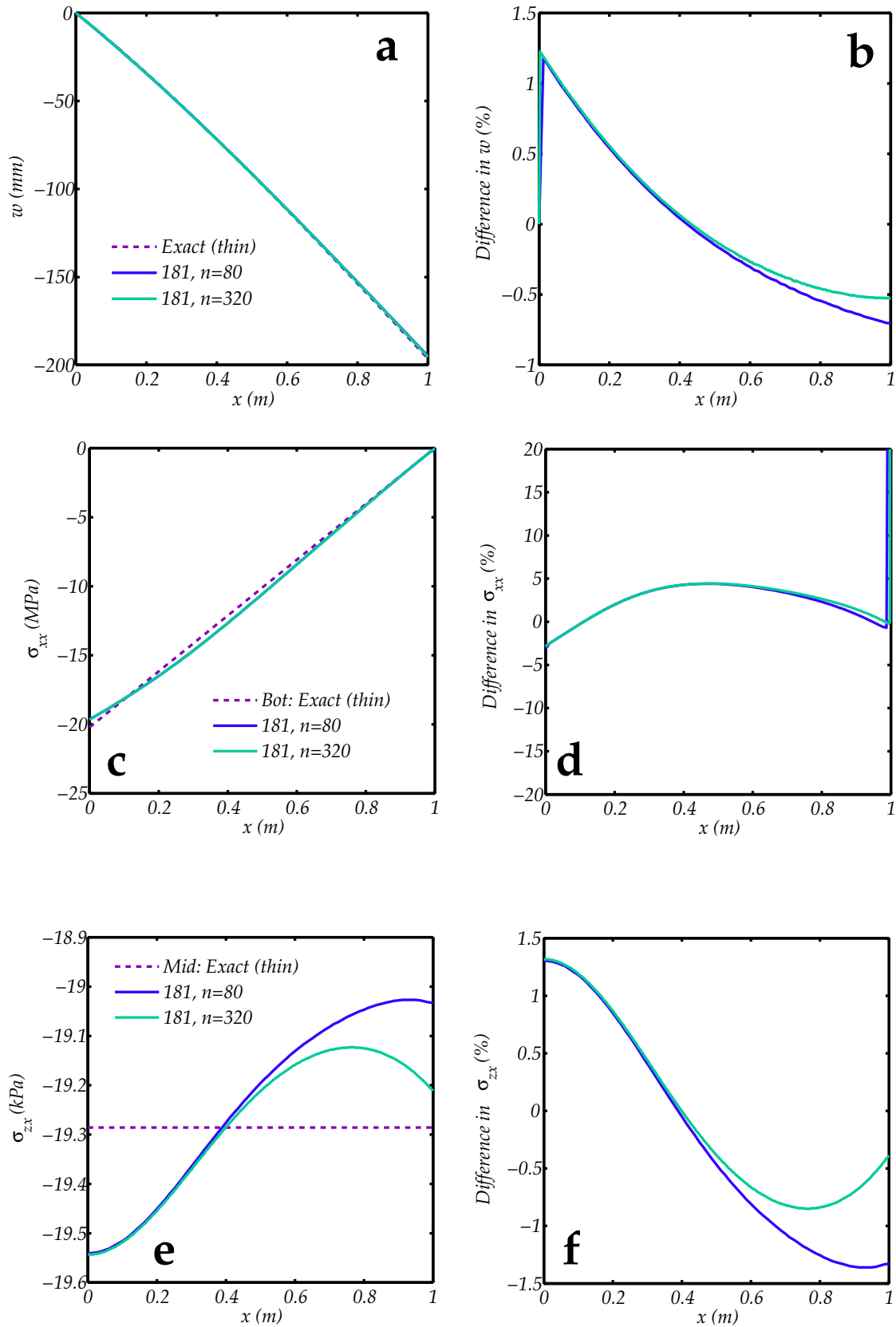
Figure 20 – *Displacement and stresses in a 22 mm thick cantilever sandwich plate under concentrated edge load. SHELL181 elements have been used for the simulations. The "exact" solution is the* thin-facesheet *approximation for a sandwich beam.*
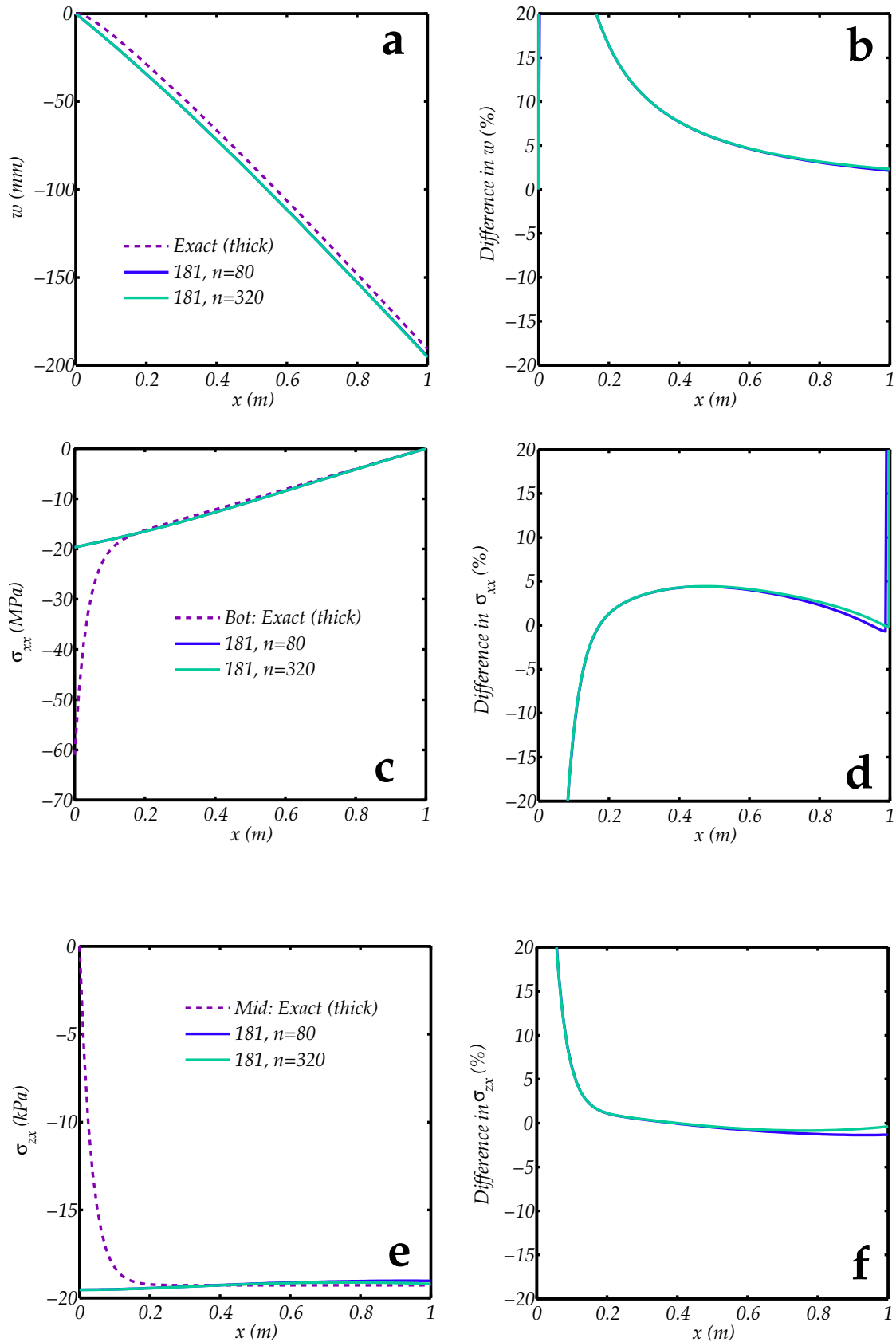
Figure 21 – *Displacement and stresses in a 22 mm thick cantilever sandwich plate under concentrated edge load modeled with SHELL181 elements. The "exact" solution is the* thick-facesheet *solution for a sandwich beam.*
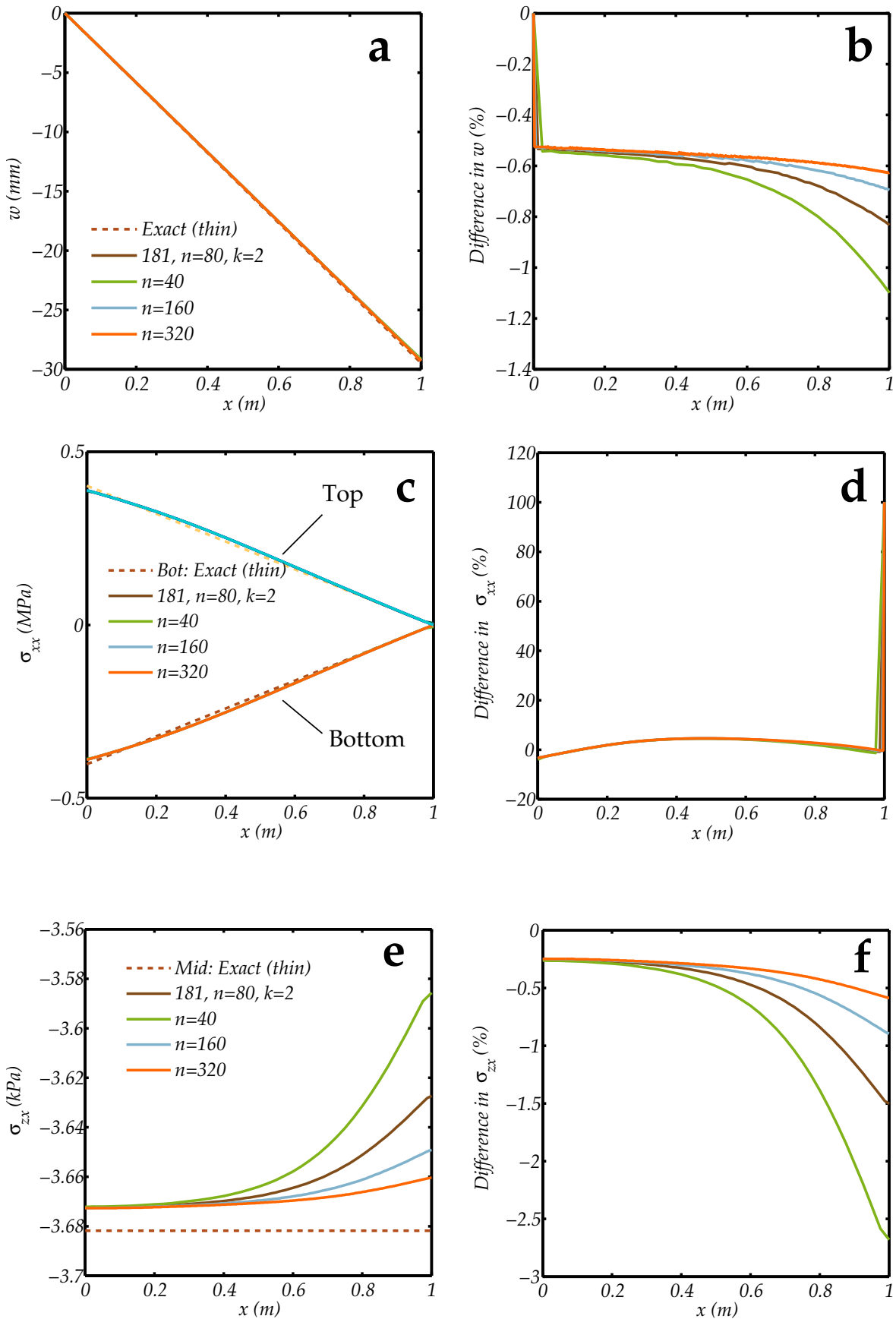
Figure 22 – *Displacement and stresses in a 12 cm thick cantilever sandwich plate under concentrated edge load modeled with SHELL181 elements. The "exact" solution is the thick-facesheet solution for a sandwich beam.*
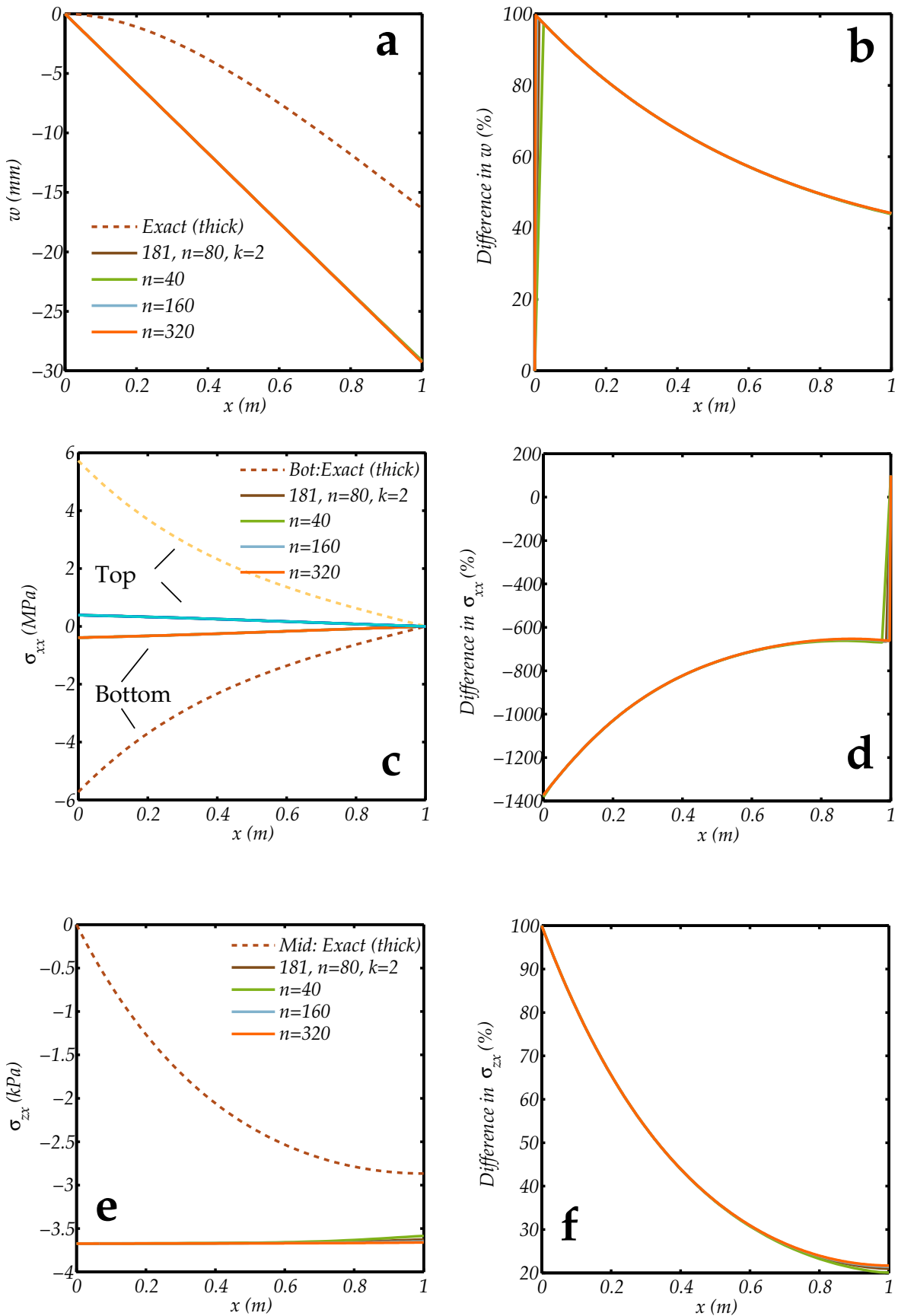
Figure 23 – *Displacement and stresses in a 12 cm thick cantilever sandwich plate under concentrated edge load modeled with SHELL181 elements. The "exact" solution is the thick-facesheet solution for a sandwich beam.*

6.3 SOLSH190 element

In contrast with the SHELL181 element, the SOLSH190 element behaves more like a sandwich shell with thick facesheets and matches the thick-facesheet solution quite accurately. Since the thick-facesheet solution is more accurate, we will only compare the ANSYS$^{\text{TM}}$ results with that solution. The displacement and stresses predicted by SOLSH190 elements are compared with the thick-facesheet solution and the SHELL181 solution in Figure 24 (p. 40). All SOLSH190 simulations except one were performed with three elements through the thickness.

Several different boundary conditions have been explored in our study. The asymmetry between the bending stresses at the top and bottom of the panel (observed in isotropic and orthotropic cantilever plates) was found to be caused by the positioning the load to act only on the top surface of the plate. If, instead, the load was applied so that half was at the top and half at the bottom, the asymmetry disappeared. The results shown in Figure 24 have all been obtained using loads applied both at the top and the bottom of the plate at the loaded edge. The displacement boundary conditions at the clamped edge also have a strong effect on the results. Several boundary conditions have been explored; the results from three types of applied displacement are shown in the figure. These are $bc = 0$, where the degrees of freedom of all nodes at the clamped edge are fixed; $bc = 2$, where only nodes at the mid-planes of the facesheets and core are fixed; and $bc = 4$ where the top node of the top facesheet, the bottom node of the bottom facesheet, and the mid-plane node of the core are fixed at the clamped end.

Parts a and b of Figure 24 show the displacements predicted when SOLSH190 elements are used. The significant outlier corresponds to the case where one element is used through the thickness of the sandwich ($e = 1$). This element has three layers; the two outer layers correspond to the facesheets and the inner layer is the core. Clearly, the element is excessively stiff and therefore inadequate. If we now examine the SHELL181 solution in blue, we observe that it is close to the SOLSH190 with the $bc = 2$ option. This boundary condition poorly constrains the clamped edge and therefore cannot be an accurate representation of a clamped boundary condition. The fact that the SHELL181 solution is identical to the SOLSH190 solutions with extremely compliant boundary conditions is further indication that these solutions cannot be accurate. Notice that the fully clamped solution ($bc = 0$) and the clamped facesheet with partially clamped core ($bc = 4$) lead to results that are very close to the thick-facesheet exact solution. Convergence is also rapid as seen from the overlapping curves for 80 elements and 320 elements along an edge.

The plots of bending stress shown in parts c and d of the figure are also further illustrative of the accuracy of the SOLSH190 calculations. With a properly constrained clamped edge, the SOLSH190 element predicts stresses that are identical to the thick-facesheet exact value, even at the clamped edge where the stress increases significantly. However, the SHELL181 and SOLSH190 with $bc = 2$ predict much lower stresses at the clamped edge.

If we examine the transverse shear stresses in parts e and f of the figure, we notice that SOLSH190 calculations with one element (containing three layers) through the thickness overestimate the stress significantly. However, with the correctly constrained clamped edge and three elements (each containing one layer) through-thickness, the SOLSH190 solutions are almost identical to the exact, thick-facesheet, solution. The large difference close to the clamped edge observed in part f of the figure is due to the large gradient in the stress close to that edge. Clearly, the fact that the thick-facesheet solution is matched well by SOLSH190 elements indicates that these elements are more accurate than SHELL181 elements.

Similar results are observed for the thicker panel in which the thick-facesheet solution and the SOLSH190 solution are quite close as can be observed in Figure 25 (p. 42). The SOLSH190 results shown in the figure are from calculations with three elements through the thickness ($e = 3$) and with the load applied on both the top and bottom nodes of the panel at the loaded edge ($load = 2$).
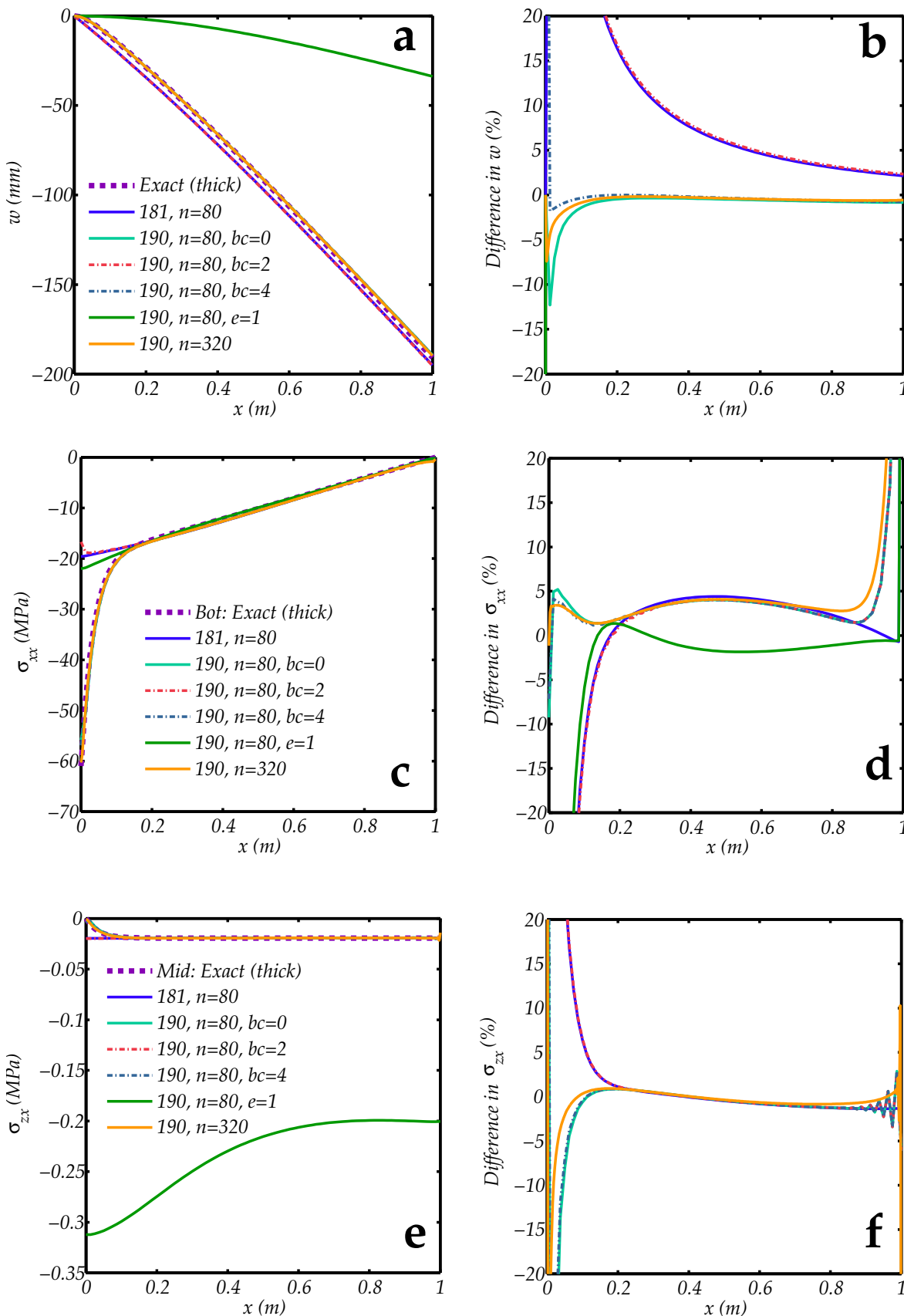
Figure 24 – *Displacement and stresses in the thin cantilever sandwich plate under concentrated edge load modeled with SOLSH190 elements. The "exact" solution is the thick-facesheet approximation. The SHELL181 solution with 80 elements along an edge has also been shown for comparison.*

The SOLSH190 results shown in cyan are an exception in that they correspond to the situation where the load is applied only to the top edge of the panel ($load = 1$).

The displacements along $y = 0$ are shown in parts a and b of the figure. The SHELL181 solution and the SOLSH190 solution with $bc = 2$ are identical, and certainly wrong. All the other SOLSH190 results match the thick-facesheet exact solution well. In fact, as seen in part b of the figure, the best match is for the case where all nodes at the clamped end are fixed ($bc = 0$).

If we examine the bending stresses in parts c and d of the figure, we once again see that the SOLSH190 simulation with fully clamped nodes ($bc = 0$), and loaded both on the top and the bottom ($load = 2$), matches the exact thick-facesheet solution best. The stresses predicted by SHELL181 elements (and SOLSH190 with $bc = 2$) are far too low. A partially clamped core, $bc = 4$, shows large fluctuations near the clamped edge and a top loaded plate ($190, n = 80, e = 3$) shows an asymmetry between the top and bottom facesheets (note that the top facesheet solutions are not shown in the plots).

The transverse shear stress solutions in parts e and f of the figure show similar trends. The $load = 2, bc = 0$ case matches the exact solution perfectly except in a region close to the clamped edge. The discrepancy has been tracked down to the way in which ANSYS$^{\text{TM}}$ interpolates results to a PATH when the PDEF command is used with the NOAVG option.

These results further confirm the accuracy of SOLSH190 elements relative to SHELL181 elements.

6.4   SOLID185 element

The exact solution can be checked by modeling the plate with three-dimensional SOLID185 elements and comparing the results. Figure 26 (p. 43) shows one such set of comparisons. In the figure, SOLID185 simulations with clamped mid-planes only ($bc = 2$) and fully clamped facesheets($bc = 4$) are compared with the thick-facesheet exact solution, the SHELL181 solution, and SOLSH190 solutions with partially or fully clamped facesheets ($bc = 2$ or $bc = 4$). In the SOLID185 calculations each facesheet has been modeled with four through-thickness elements and the core has 20 through-thickness elements. Also, the SOLID185 calculations use the enhanced assumed strain element formulation.

The displacement solution and the difference between ANSYS$^{\text{TM}}$ results and the exact (thick-facesheet) solutions are plotted in parts a and b of the figure. When only the mid-planes of the facesheets and core are clamped, the SOLID185, SOLSH190, and SHELL181 solutions are identical and match the thin-facesheet solution. On the other hand, when the facesheets are clamped, though the SOLID185 and SOLSH190 solutions are identical, they are closer to the more accurate thick-facesheet solution. These results indicate that SOLID185 and SOLSH190 elements behave identically and, with the correct boundary conditions, are more accurate than SHELL181 elements.

Parts c and d of the figure show the bending stresses at the bottom of the sandwich plate. Once again, we see that SOLID185 and SOLSH190 elements behave identically and, when appropriately clamped, match the exact solution very well. The same behavior is seen in parts e and f of the figure which depict the transverse shear stresses at the mid-surface of the plate along $y = 0$. These results confirm that SOLSH190 elements are superior to SHELL181 elements for modeling sandwich panels with isotropic facesheets and cores.
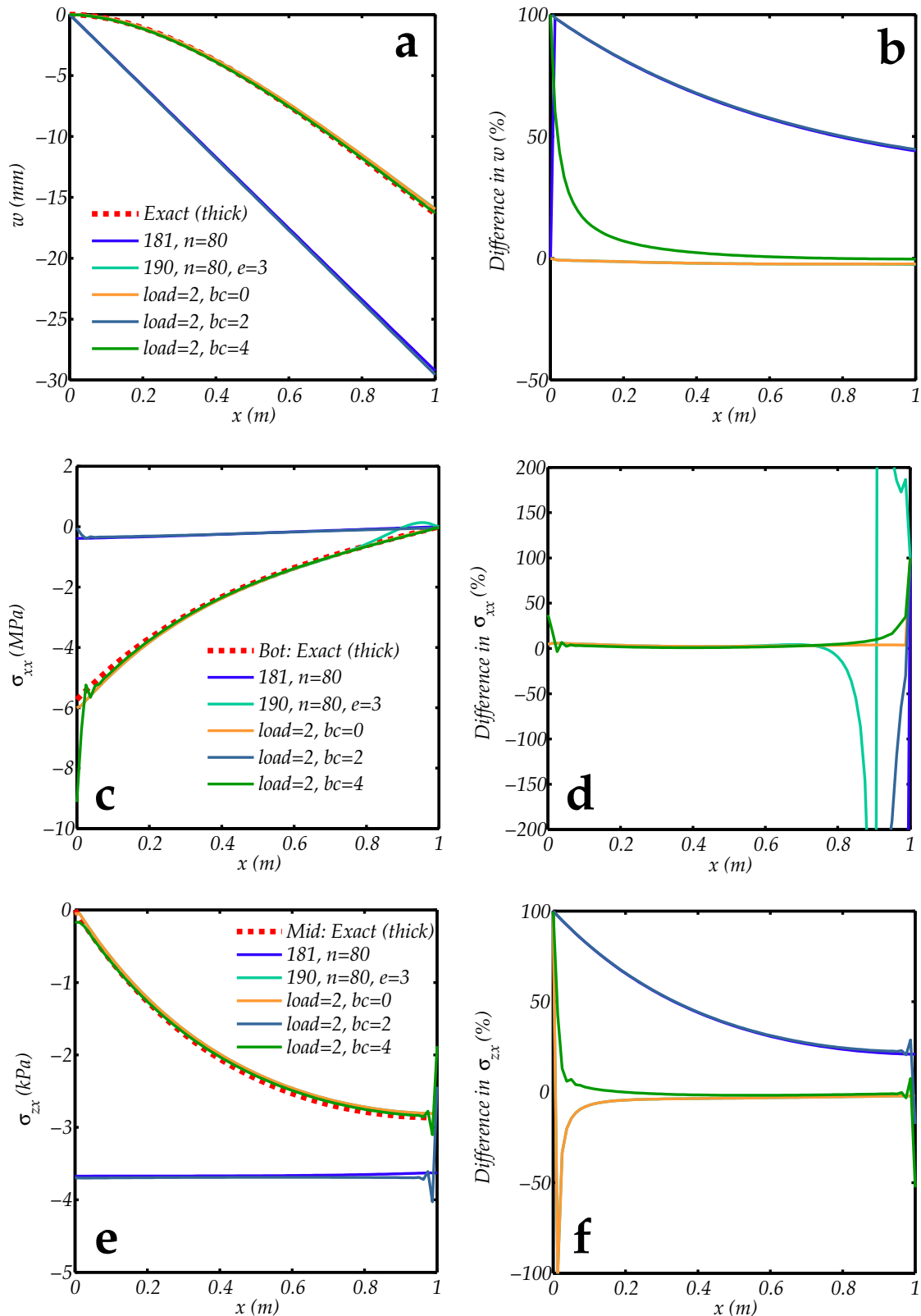
Figure 25 – *Displacement and stresses in the 12 cm thick cantilever sandwich plate under concentrated edge load modeled with SOLSH190 elements. The "exact" solution is the thick-facesheet approximation. The SHELL181 solution with 80 elements along an edge has also been shown for comparison.*
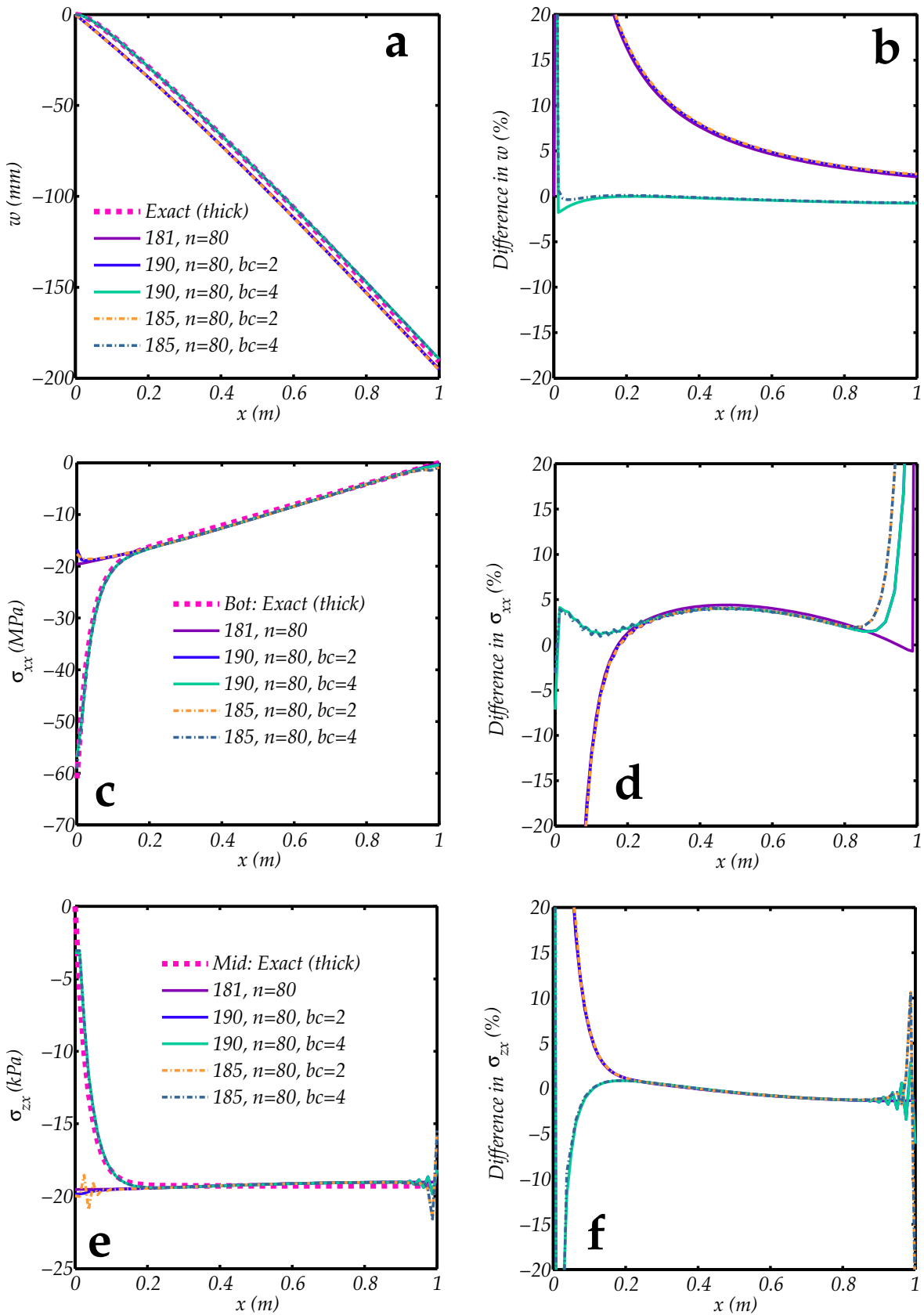
Figure 26 – *Displacement and stresses in a 22 mm thick cantilever sandwich plate under concentrated edge load. The "exact" solution is the thick-facesheet approximation. The plots contain results from simulations with SOLID185, SHELL181, and SOLSH190 elements.*

7   Cantilevered anisotropic sandwich plate with concentrated edge load

Exact solutions for cantilevered plates composed of orthotropic materials are difficult to calculate. However, the results of the previous section have shown that SOLID185 calculations can give quite accurate results. Therefore, in this section, we use SOLID185 simulations to determine the baseline results against which SHELL181 and SOLSH190 are compared. Exact results for sandwich composites with isotropic components are also provided.

As before, a square sandwich panel of planar dimensions 1 m × 1 m is simulated. The thickness of the panel is 22 mm (two facesheets 1 mm thick and a core 20 mm thick). The total applied force is 405 N. The material properties of the facesheets are are $E_{xx} = E_{yy} = 17.3$ GPa, $E_{zz} = 3.24$ GPa, $G_{xy} = 6.7$ GPa, $G_{yz} = G_{zx} = 1.2$ GPa, $\nu_{xz} = \nu_{yz} = 0.32$. The core is considerably less stiff with $E_{xx} = 0.34$ MPa, $E_{yy} = 0.48$ MPa, $E_{zz} = 132$ MPa, $G_{xy} = 4.55$ MPa, $G_{yz} = 24.1$ MPa, and $G_{zx} = 41.4$ MPa. The Poisson's ratios of the core are $\nu_{xy} = 0.49$, $\nu_{xz} = 0.01$, and $\nu_{yz} = 0.01$. Simulations have shown that interchanging these Poisson's ratios with minor Poisson's ratios do not affect the results significantly.

Figure 27 shows the two situations simulated in this section. The first involves a cantilevered sandwich plate subjected to an edge load of the same magnitude as that in Section 6. The displacements and rotations of the clamped edge of the plate are set to zero. The second situation involves an additional wall to which the sandwich plate is fixed. The wall is composed of SOLID185 elements. The load is the same as for the first case.
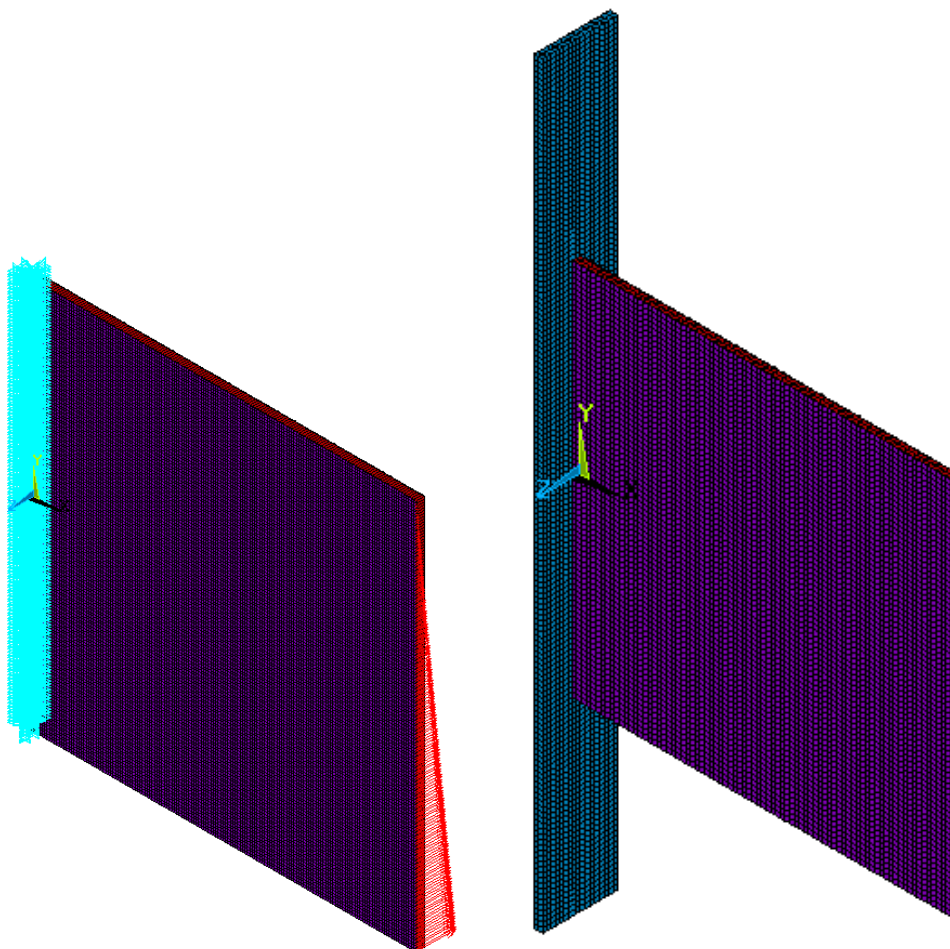

Figure 27 – *Models of anisotropic sandwich plates under concentrated edge load.*

7.1 SHELL181 element

Figure 28 (p. 46) shows the displacements and stresses in the plate when modeled with SHELL181 elements. The surprising feature of these results is that the SHELL181 solution almost exactly matches the SOLID185 solution (recall that for sandwich panels with isotropic facesheets and core, there was a small but significant difference between SOLID185 and SHELL181 solutions). Switching the Poisson's ratios from major to minor ($pr = 2$) does not affect the solution significantly. If we change the orientation of the axes of orthotropy of the core ($or = 45$ or $or = 90$) in the plane of the plate, some small differences are observed but these are not large enough to have a significant effect on the peak stresses. The percent differences shown in the figure are relative to the SOLID185 solution. We also observe that the SOLID185 solution is noisy at the clamped and loaded edges.

These results show that SHELL181 produce accurate results for relatively thin sandwich composites with orthotropic facesheets and core when the core transverse shear stiffness is relatively large compared to the in-plane shear stiffness. This result is strange and suggests that some tuning has been applied to the ANSYS$^{\text{TM}}$ SHELL181 element so that it produces the right behavior for such sandwich composites.

7.2 SOLSH190 element

If we examine the response of SOLSH190 elements under the same conditions (see Figure 29, p. 47) we observe that when three ($e = 3$) or six ($e = 6$) elements are used through the thickness, the displacements and stresses are close to the SHELL181 and SOLID185 solutions. Convergence is also rapid. However, the SOLSH190 displacement and transverse shear stress differ significantly from the SOLID185 solution when only one element (with three layers) is used through the thickness. The noisy nature of the percentage difference plots is because of the noisy SOLID185 solution at the edges of the plate and local refinement is required to improve the solution in these regions.

7.3 Wall attachment

When the plate is attached to a wall made of SOLID185 elements, more preprocessing is required to make sure that nodes on the plate match up with nodes on the wall. For a SHELL181 element this process is relatively straightforward. The solid wall has to be partitioned so that it contains a line that matches the attached edge. The edge is then attached to the wall by setting the rotational degrees of freedom at the nodes along the shared line to zero. When the plate is modeled using SOLSH190 elements, the partitioning needed is more complex. The first step is to partition the geometry so that the area shared by the wall and the plate is represented as a domain in the plate. The plate is next meshed so that it has either one element (with three layers) or three elements through the thickness. The wall is meshed last so that the discretization of the plate is transferred to it. This process leads to matching nodes on the wall and plate and further boundary conditions at the clamped edge of the plate are not necessary. A similar process is needed when the plate is modeled with SOLID185 elements.

Figure 30 (p. 48) shows the displacements and stresses for the situation where the sandwich plate is attached to a wall. Once again we see that if we model the plate with one through-thickness SOLSH190 element ($e = 1$), the results are not accurate. Excellent agreement with the SOLID185 solution is found when SHELL181 or SOLSH190 elements (with three or six through-thickness elements) are used.
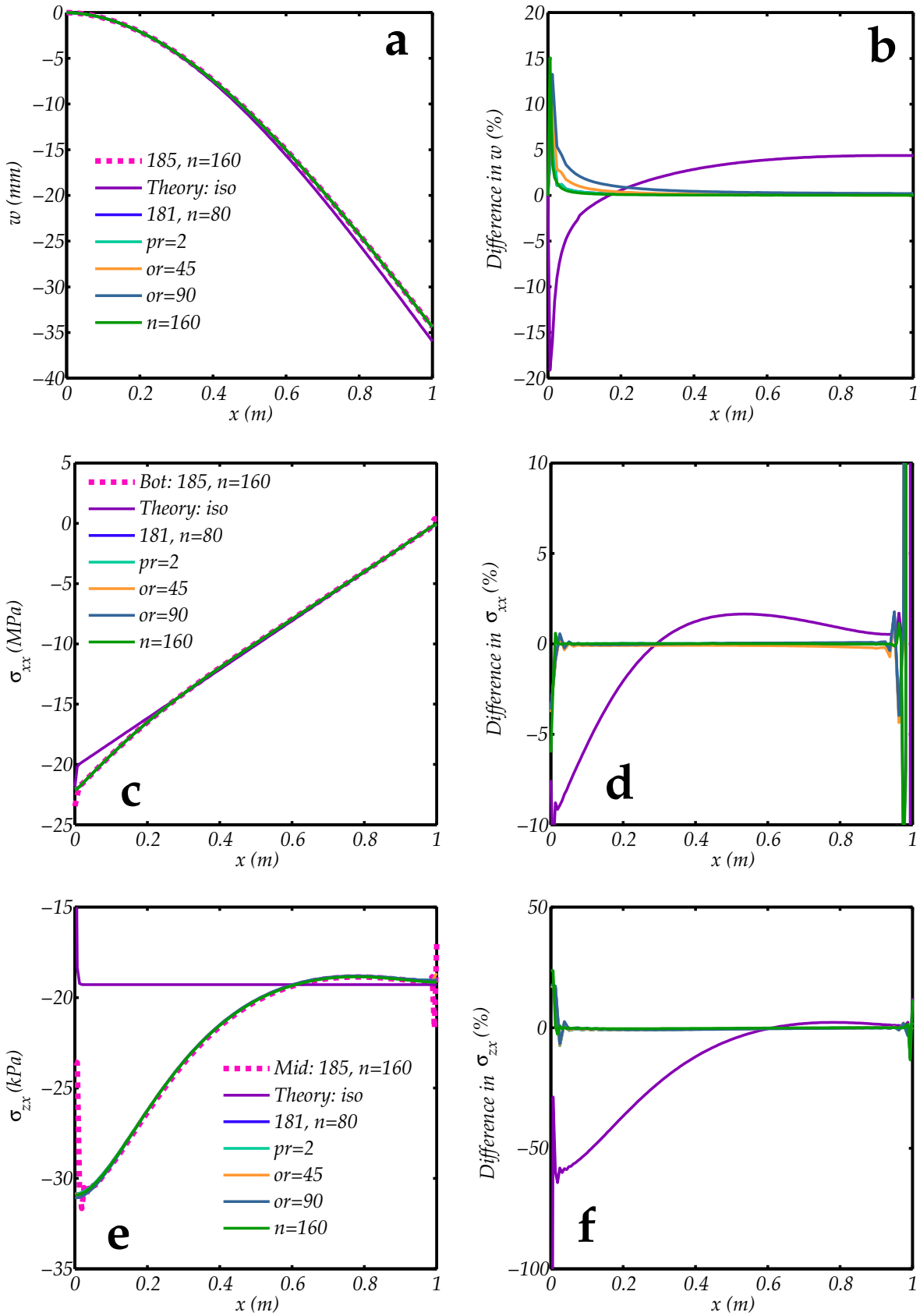
Figure 28 – *Displacement and stresses in a thin orthotropic cantilever sandwich plate modeled with SHELL181 elements under a concentrated edge load.*
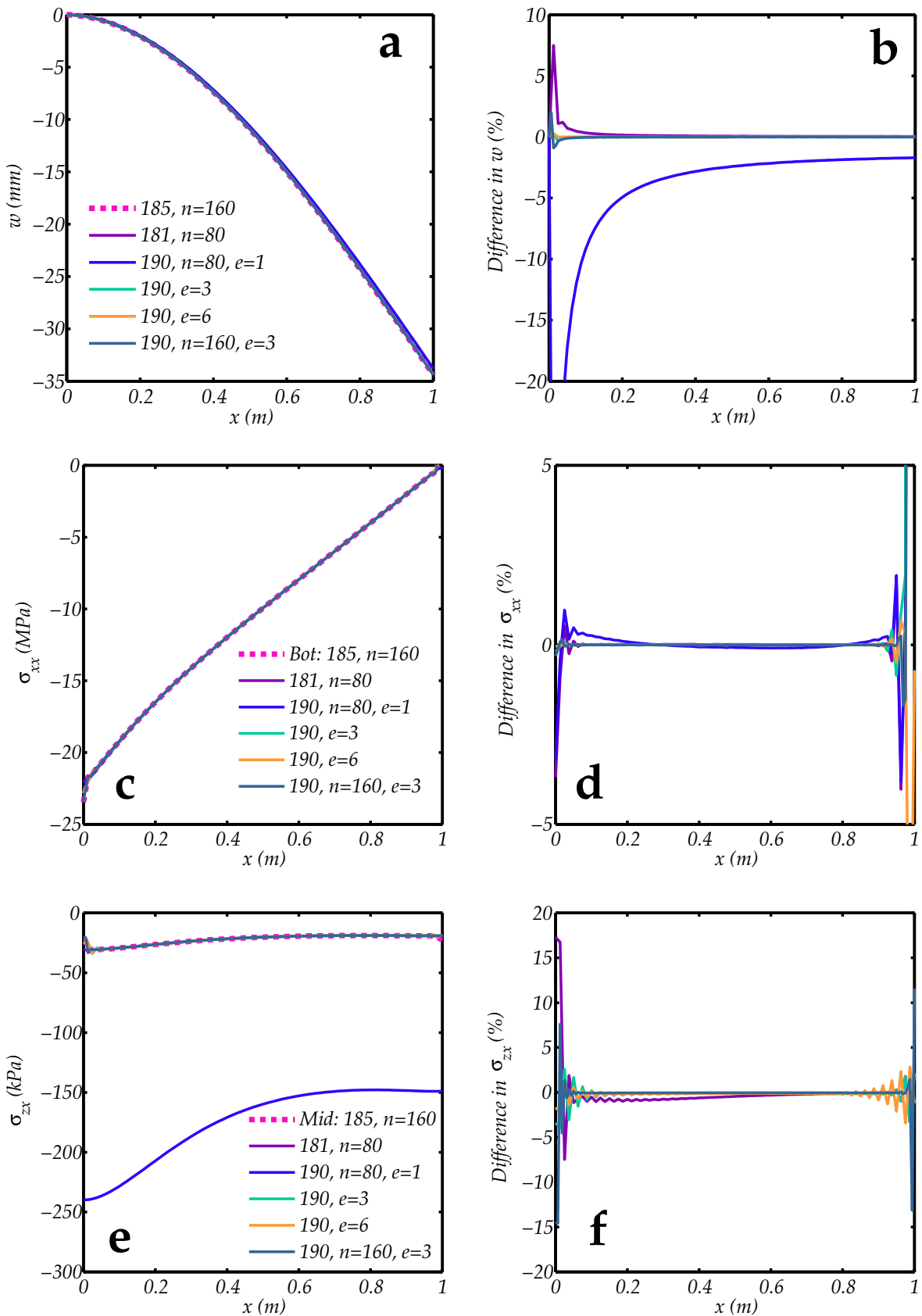
Figure 29 – *Displacement and stresses in a thin orthotropic cantilever sandwich plate under concentrated edge load.*
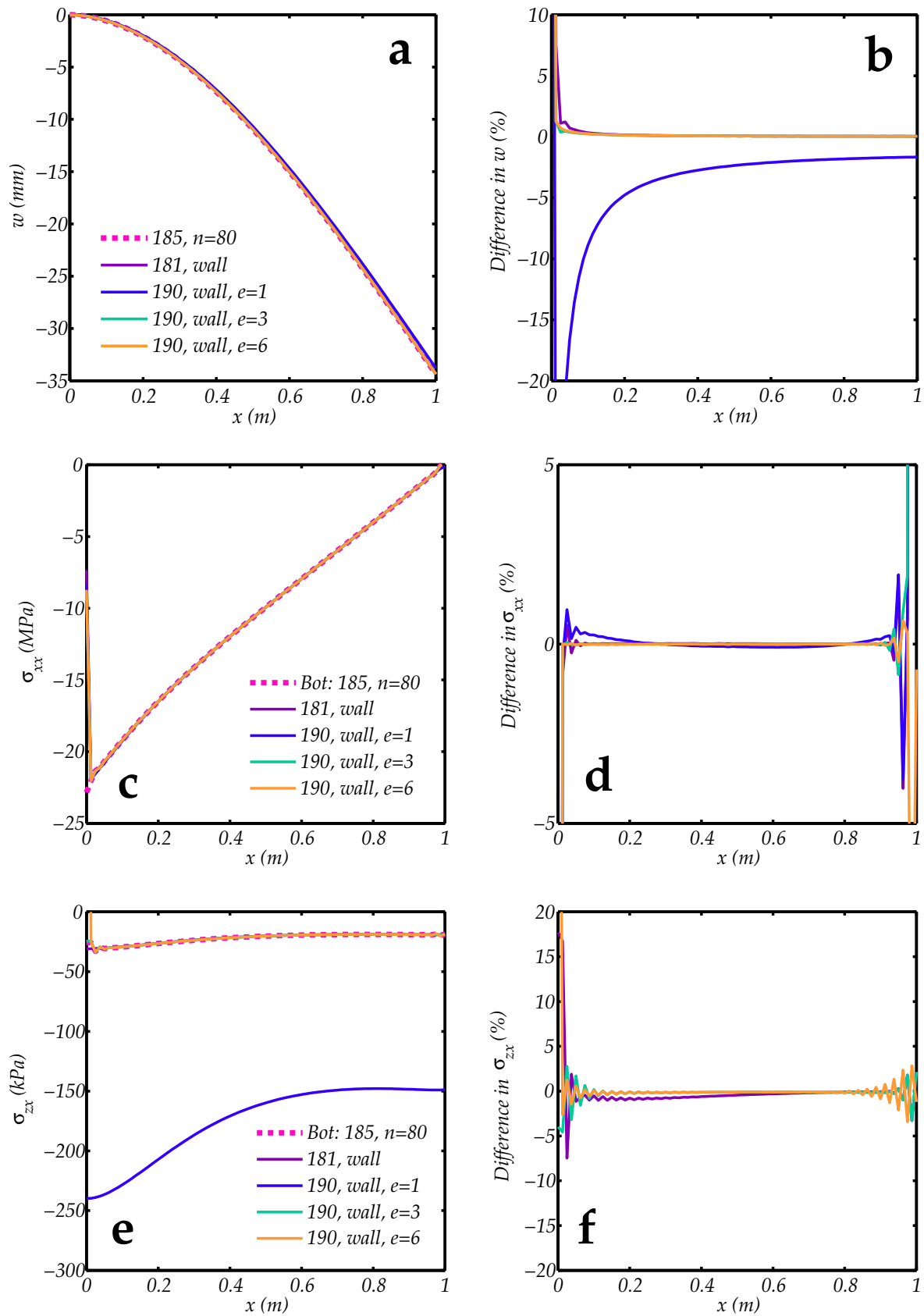
Figure 30 – *Displacement and stresses in a thin orthotropic cantilever sandwich plate that is attached to a wall and loaded by a concentrated edge.*

8 Cantilevered anisotropic sandwich plate under acceleration load

Another situation of interest is when a cantilevered anisotropic plate is loaded by a body force due to a downward acceleration of $9g$. The plate has dimensions and material properties identical to those used in the previous section. Plates modeled with SOLSH190 and SOLID185 elements were clamped by fixing the displacements of all nodes along the clamped edge to zero. Figure 31 (p. 50) shows the displacement and stresses in the plate when different element types are used.

The displacements plotted in parts a and b of the figure are nearly identical when SOLID185, SHELL181, and SOLSH190 elements (with three through-thickness elements) are used. The outlier in light green is for the case where SOLSH190 elements were used with one element through the thickness and three layers in each element.

The bending stresses in parts c and d of the figure differ slightly from the SOLID185 solution at the free edge. The closest solution is obtained when SOLSH190 elements with three through-thickness elements are used. The same behavior is observed in the transverse shear plots shown in parts e and f of the figure.

It can be concluded that SHELL181 elements and SOLSH190 elements both give reasonable results when an accleration-based body force is applied.
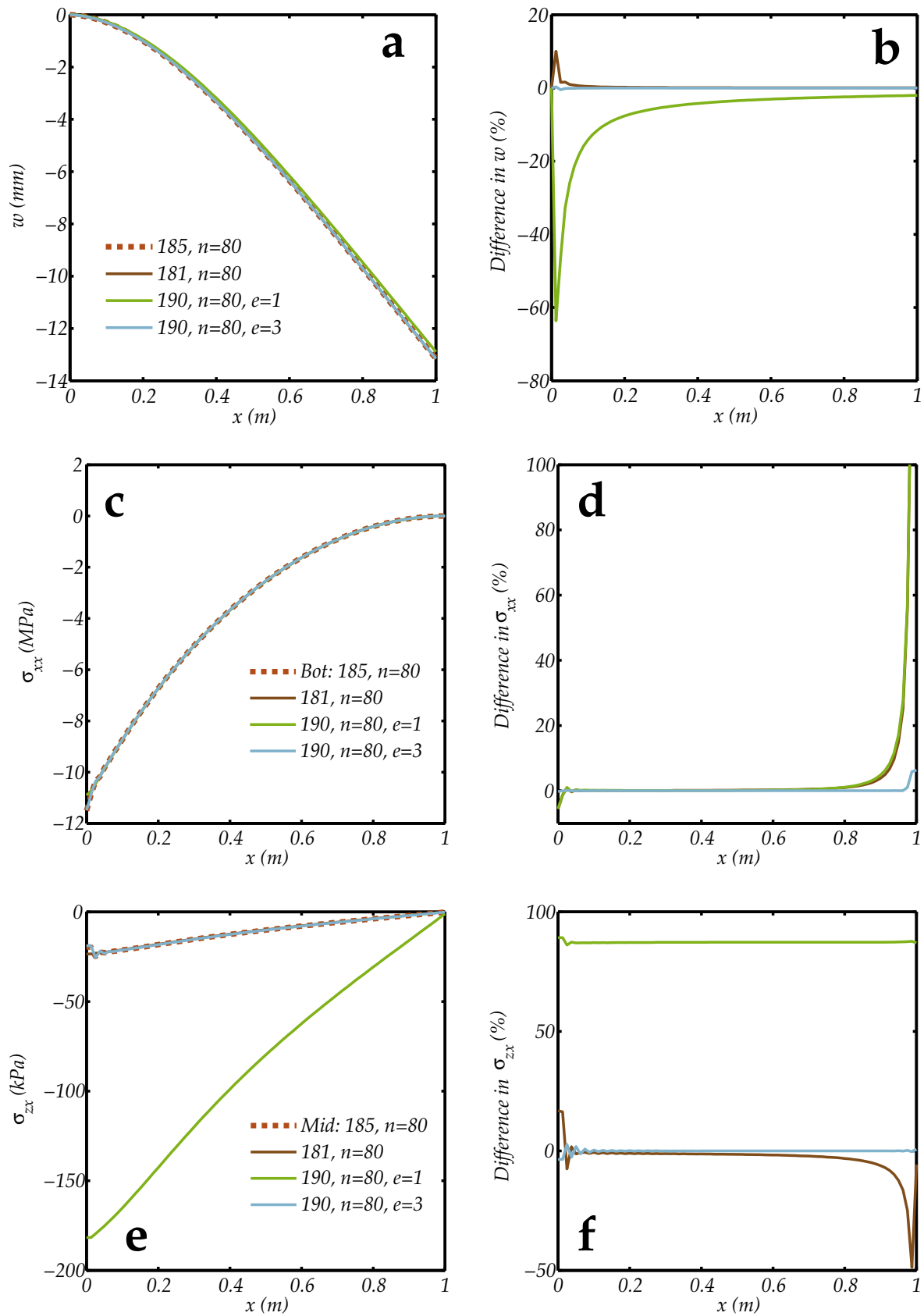
Figure 31 – *Displacement and stresses in a thin orthotropic cantilever sandwich plate under 9 g acceleration load.*

9 Summary

Several situations have been examined in this study with variations in plate geometry, boundary conditions, and material properties. The following summarizes the findings of the study.

- Both SHELL181 and SOLSH190 elements appear to be more compliant that expected from thin plate theory for isotropic plates. Plates that have a thickness that is 1/25 the planar dimensions appear to be too thick for Kirchhoff-Love theory to be applicable.

- Convergence is rapid and around 80 elements per meter seems to be sufficient for a 1 m × 1 m plate that is 1/25 m thick. This number can be used as a rule of thumb for other plate sizes.

- The number of integration points through the thickness does not appear to affect the solution as long as the number is three or greater.

- The choice of KEYOPT(3) in SHELL181 elements does not affect the results in any of the loading scenarios examined in this study.

- At least three SOLSH190 elements should be used through the thickness for accurate results. A single element with three layers in not adequate for most situations. This is problematic because certain versions of ANSYS Workbench$^{\text{TM}}$ appear not to allow three adjacent layers if SOLSH190 elements.

- Simulations of thin structures with SOLID185 elements should use the enhanced strain option (KEYOPT(2)=2) and, at least three elements through the thickness of each component in a sandwich structure, to avoid locking behavior and for accurate results.

- Loads and displacements have to be applied on both sets of nodes in SOLSH190 elements (i.e., nodes on the top and bottom of the mid-surface) to achieve behavior that is identical to that of SHELL181 elements.

- Care should be taken when using SHELL181 elements to model sandwich composites with isotropic core/facesheet. To check that the correct results are being obtained, a few comparisons with SOLID185 elements with enhanced strain should be completed.

- Both SHELL181 and SOLSH190 elements perform adequately for sandwich composites with material properties and geometries similar to those used in the aerospace industry, provided care is taken to apply the correct boundary conditions when using SOLSH190 elements.

Acknowledgments

References

[1] S. Timoshenko and S. Woinowsky-Krieger. *Theory of plates and shells*. McGraw-Hill, New York, 1959. 5, 15

[2] R. D. Mindlin. Influence of rotatory inertia and shear on flexural motions of isotropic, elastic plates. *ASME Journal of Applied Mechanics*, 18:31–38, 1951. 5

[3] C. M. Wang, G. T. Lim, J. N. Reddy, and K. H. Lee. Relationships between bending solutions of reissner and mindlin plate theories. *Engineering Structures*, 23:838–849, 2001. 5

[4] G. T. Lim and J. N. Reddy. On canonical bending relationships for plates. *International Journal of Solids and Structures*, 40:3039–3067, 2003. 5

[5] E. Reissner and M. Stein. Torsion and transverse bending of cantilever plates. Technical Note 2369, National Advisory Committee for Aeronautics, Washington, 1951. 20

[6] D. Zenkert. *An Introduction to Sandwich Construction*. EMAS, London, 1995. 33

[7] F. J. Plantema. *Sandwich Construction*. John Wiley and Sons, New York, 1966. 33